I. Emri, Rheology Reviews 2005, pp 49 - 100.

RHEOLOGY OF SOLID POLYMERS

Igor Emri

Center for Experimental Mechanics, Faculty of Mechanical Engineering
University of Ljubljana, 1125 Ljubljana (SLOVENIA)

ABSTRACT

The mechanical properties of solid polymeric materials quite generally depend on time, i.e., on whether they are deformed rapidly or slowly. The time dependence is often remarkably large. The complete description of the mechanical properties of a polymeric material commonly requires that they be traced through 10, 15, or even 20 decades of time. The class of polymeric materials referred to as thermo-rheologically and/or piezo-rheologically simple materials allows use of the superposition of the effects of time and temperature and/or time and pressure in such materials as a convenient means for extending the experimental time scale.

This paper presents a critical review of models proposed to describe the effect of temperature and/or pressure on time-dependent thermo-rheologically and/or piezo-rheologically simple polymeric materials. The emphasis here is on the theoretical aspects, although experimental results are used as illustrations wherever appropriate.

KEYWORDS: Excess enthalpy, excess entropy, FMT model, free volume, glass transitions, pressure effects, rate processes, shift functions, temperature effects, time-temperature-pressure superposition, WLF model

1. INTRODUCTION

Polymeric materials exhibit time-dependent mechanical properties that can profoundly affect the performance of polymer products. The degree of change in the mechanical properties of polymeric materials over time depends on many factors. These are primarily the temperature, pressure, humidity, and stress conditions to which the material is subjected during its manufacture and during its application. Therefore, processing parameters, like pressure and temperature, play an important role in determining the quality of parts made by injection moulding, compression moulding, extrusion, etc. Unsuitable processing conditions may cause parts to warp or crack. These phenomena can occur in manufactured articles even in the absence of any mechanical loading, in particular, in the presence of high-modulus fillers. Explosions (detonations) represent special cases entailing extremely high temperatures and pressures.

The mechanical behaviour of polymeric materials is generally characterized in terms of their time-dependent properties in shear or in simple tension. The time dependence of their bulk properties is almost universally neglected (see, e.g., Kralj et al., [1]). The effect of temperature on the shear and tensile properties of polymeric materials has been fairly well understood since about the forties of the last century. By contrast, little effort went into the determination of their time-dependent bulk properties and – after initial years of activity – research on the effect of pressure lay effectively dormant. This was probably due mainly to the difficulty of making precise measurements at rather small volume deformations. The materials used in current applications simply did not appear to require a deeper understanding of the time dependence of their bulk properties and of the effect of pressure on their time-dependent shear properties to warrant exerting the exacting effort required. This situation has now changed. The demand for sustainable development[1] requires optimization of the functional and mechanical properties of new multi-component systems such as composite and hybrid materials, structural elements, and entire structures. Optimization of material use requires a much deeper understanding of the effect that temperature and pressure exert on the time dependence of the bulk as well as the shear properties of the constituents of these materials than is currently available.

Our primary focus in this paper is the effect of pressure. However, we also review the effect of temperature, essentially as necessary background. In particular, we examine whether and in what manner the effects of time and temperature, respectively, those of time and pressure, may be assumed to *superpose*. In what follows we shall therefore pay attention largely to *time*-temperature and/or *time*-pressure relations. Measurements of a linear viscoelastic response function are, however, quite often reported as a function of *frequency*. This may be either the cycles/second frequency, f, or the radian frequency, $\omega = 2\pi f$. Because $\ln t \approx -\ln f$, time and frequency are, *mutatis mutandis*, equivalent in considerations of the effects of temperature and/or pressure.

1.1 Thermo- and piezo-rheological simplicity – shift functions.

For a special class of polymeric materials, primarily single-phase, single-transition amorphous homopolymers and random copolymers, it is possible to establish *temperature* and/or *pressure shift functions* that 'collapse', as it were, the two-dimensional contour plots into a simple graph of the chosen response function as a function of the logarithmic time, usually shown as $\log t$, or the logarithmic frequency, shown as $\log \omega$ or $\log f$, recorded at a reference temperature, T_0, or pressure, P_0. Such materials are referred to as *thermo-rheologically* and/or *piezo-rheologically simple* materials.

[1] Sustainable development aims at preserving, for the benefit of future generations, the environment and the natural resources culled from it without lowering currently excepted standards of living.

Thermo-rheological simplicity requires that all response times (i.e., all relaxation or retardation times, see Tschoegl [2], p. 86), depend equally on temperature. This is expressed by the *temperature shift function:*

$$a_{T_0}(T) = \frac{\tau_i(T)}{\tau_i(T_0)}, \quad i = 1, 2, ... \qquad \ldots\ldots\ldots (1)$$

An analogous requirement applies to piezo-rheological simplicity. This demands that all that all response times depend equally on pressure and is expressed by the *pressure shift function:*

$$a_{P_0}(T) = \frac{\tau_i(P)}{\tau_i(P_0)}, \quad i = 1, 2, ... \qquad \ldots\ldots\ldots (2)$$

Thermo-rheologically simple materials allow, by definition, *time-temperature superposition*, Gross [3, 4], i.e., the shifting of *isothermal segments* into superposition to generate a *master curve*, thereby extending the time scale beyond the range that could normally be covered in a single experiment. Figure 1a shows a schematic illustrating this procedure.

Fillers and Tschoegl [5], and Moonan and Tschoegl [6] showed that piezo-rheologically simple materials permit analogous, *time-pressure superposition*, i.e., the shifting of *isobaric segments* in a similar manner. Because of the equivalence of time and frequency, shifting of isothermal (or isobaric) segments along the logarithmic frequency axis applies just as it applies to shifting along the logarithmic time axis.

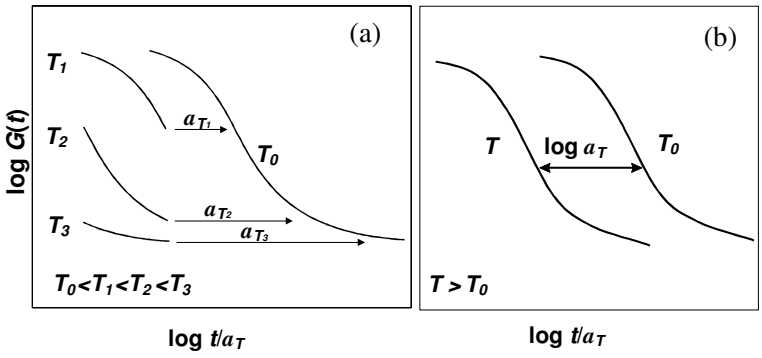

Figure 1: (a) Shifting isothermal segments into a master curve; (b) two master curves at different temperatures.

1.2 Thermo- and piezo-rheological complexity – inappropriate shifting.

The requirements embodied in equations (1) and (2) severely restrict the classes of polymers where superposition can be utilized to simplify the presentation of their physical properties. In general, superposition definitely does NOT apply to multi-phase materials such as block and graft copolymers, hybrid materials, blends, and (semi-) crystalline polymers. All these are examples of thermo-rheologically and piezo-rheologically complex materials. For reasons to be stated in section 6.2 it is doubtful whether – in the strict sense of the word – thermo and/or piezo-rheologically simple materials exist at all and, therefore, whether superposition is truly applicable even for the materials just listed. Because the class of thermo-rheologically simple materials comprises several quite important polymers, and because these dominated in the early days of the emergence of linear viscoelastic theory, it is sometimes assumed that superposability is a general feature of the mechanical properties of polymeric materials. However, thermo-rheologically and piezo-rheologically *complex* materials display two or more distinct distributions of response times, each with its own time-temperature (or time-pressure) dependence. Over limited ranges of the experimental data these 'multi-phase' materials nevertheless often seem to allow shifting of isothermal segments into superposition, generating misleading master curves.

Rusch [7] has examined the relaxation behaviour of three typical commercial ABS (acrylonitrile-butadiene-styrene) polymers. Although these were almost certainly heterogeneous, the author concluded that time-temperature superposition applied reasonably well. Such conclusions may be reached when the behaviour is viewed through an *experimental window* (the span of time or frequency within which the measurements are taken) that is simply not sufficiently wide for the lack of superposability to reveal itself (Plazek [8]; Fesko and Tschoegl [9, 10]; Kaplan and Tschoegl [11]; Cohen and Tschoegl [12]). Of course, the 'master curves' resulting from such inappropriate shifting are in error. Fesko and Tschoegl [9] have developed a procedure for the time-temperature superposition of two-phase materials. Another procedure was proposed, more recently, by Brinson and Knauss [13, 14]. However, the mechanical responses of the constituent homopolymers and their temperature functions must be known and this, in effect, begs the point at issue. The matter has been examined through computer simulations by Caruthers and Cohen [15].

1.3 Glass transition temperature and glass transition pressure.

Superposition is intimately linked with the concept of the glass transition phenomenon in polymers. Shen and Eisenberg [16] compiled an early, exhaustive review of the glass transition resulting from a change in *temperature*. This transition is characterized by the so-called glass *transition temperature*, T_g, which, by definition, is that temperature below which the micro-Brownian thermal motion of the polymer chain segments effectively ceases, i.e., slows down to such an extent that the segmental rearrangements cannot be followed experimentally. It may be defined operationally as shown in figure 2, taken from Moonan and Tschoegl [17].

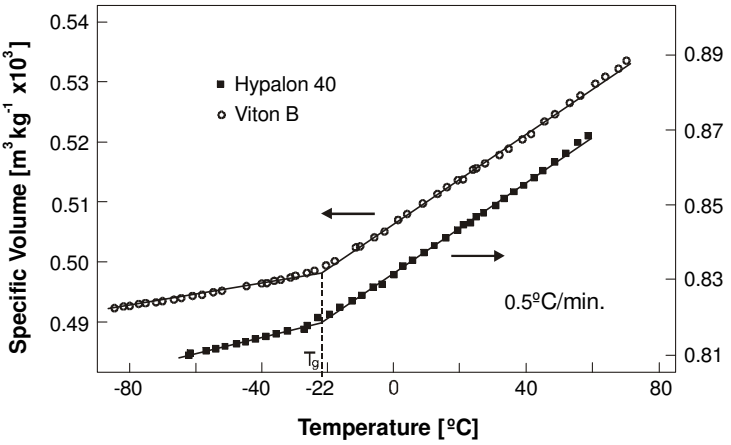

Figure 2: Operational definition of T_g

The figure shows T_g obtained from the intersection of a plot of the specific volume against the temperature, here for two rubbers having the same T_g. As determined experimentally, the glass transition temperature is a kinetic phenomenon that, however, shows many of the formal aspects of a second-order thermodynamic phase transition.

Below T_g the polymer is not in equilibrium, metastable or otherwise. A certain amount of entropy is 'frozen in' as a consequence of the tremendous loss of chain mobility that prevents the detection of segmental rearrangements on any finite experimental time scale. Thus, Nernst's heat theorem (see, e.g., Tschoegl [18], p. 47), which requires the entropy to vanish at the absolute zero of temperature, is not obeyed. DiMarzio and Gibbs [18, 21, 22] have shown that it is possible to postulate the existence in polymers of a second-order thermodynamic transition temperature, T_2, that could, however, be reached only by an infinitely slow cooling process. For reasons to be stated in section 2.7 we shall designate this temperature as the 'threshold' temperature and assign the symbol T_L to it. The glass transition temperature depends on pressure, and this has been noted by several authors (see, e.g., Paterson [26], Bianchi [27]).

In analogy to the glass transition temperature, $T_g(P)$, there exists also a *glass transition pressure*, $P_g(T)$, above which the micro-Brownian motion of the polymer chain segments ceases. Above P_g a polymer is again not in thermodynamic equilibrium for the same reason that is not in equilibrium below T_g. One may postulate that in polymers there exists also a second-order thermodynamic phase transition pressure, P_2 (or P_L), but nothing seems to be known about it at this time, except its existence. Temperature would presumably affect the glass transition

pressure but data on this phenomenon also appear to be lacking. Being kinetic rather than thermodynamic phenomena, the glass transitions depend on the time rate at which they are determined. They are actually narrow *ranges* rather then specific temperatures or pressures. Superposition requires that the material be in thermal and mechanical equilibrium. In order to reach the equilibrium in a relatively short period of time, material must therefore be above the glass transition temperature, T_g , and/or below the glass transition pressure, P_g .

1.4 Purpose and scope of the article.

Despite the reservations expressed in the previous sections, superposition has been and is being used widely. The literature on the effect of temperature on the mechanical properties of polymeric materials is extensive. That on the effect of pressure is less so. This article presents a review of what has been done to date in modelling temperature and/or pressure shift functions for polymeric materials in equilibrium with respect to temperature and pressure. Two papers concerned solely with the effect of pressure on the viscosity of non-polymeric liquids, e.g., Matheson [28], have not been reviewed.

Our discussion will be facilitated by recognizing certain regions of the linear viscoelastic response functions. Those that one records on *crosslinked* materials (e.g., rubbers) exhibit three distinct regions: the glassy, the transition, and the rubbery region. In *uncrosslinked* materials there exist four: the glassy, the transition, the plateau, and the flow region. Figure 3 displays a schematic of these regions. We initially consider the effect of temperature and pressure on the transition region of amorphous, isotropic, homogeneous materials. This region is commonly referred to as

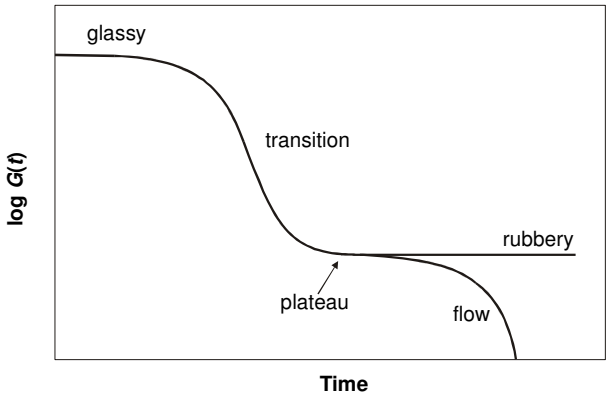

Figure 3: Schematic displaying the distinct regions of crosslinked and uncrosslinked materials.

the 'main' transition region to distinguish it from possible other transitions (see section 6.2. The scope will be widened in sections 6, 7, and 8 to include the other regions of the linear viscoelastic response. We shall consider primarily deformation in shear. Brief reference will be made to other types of deformation in section 9, and to anisotropic materials in section 10. In sections 2, 3, and 4 we will introduce various models describing the effect of temperature and pressure on the mechanical properties of thermo- and/or piezo-rheologically simple polymeric materials. Each section will contain a critique of these models. These critiques will be deferred, however, until the models in each section have all been introduced. We shall further attempt also to point out – to the best of our understanding – areas where information on the effect of temperature or pressure on the mechanical properties of thermo- and/or piezo-rheologically simple materials is currently lacking.

2. MODELLING THE EFFECT OF TEMPERATURE

The effect of temperature on the time-dependent mechanical properties of polymers is relatively well understood although a number of problems remain open. Above T_g it is generally modeled by the well-known WLF equation, named after its originators, Williams, Landel, and Ferry. We review the derivation and properties of this equation as necessary background to our discussion of the effect of pressure. The WLF equation is concerned with the relaxation or retardation behaviour arising from the micro-Brownian (or segmental, or backbone) motion of the polymer chains. It has been derived from consideration of the fractional free volume. However, equations of the same form have been proposed also by considering the relaxation or retardation process as the physical counterpart of a chemical reaction, or by considering changes in the excess (configurational) entropy[2], or in the excess enthalpy. While all these approaches lead to equations of the same form, the empirically obtained parameters of the equation are interpreted differently.

2.1 The Doolittle equation.

Many theories for modelling the effect of thermodynamic parameters such as temperature or pressure on the time-dependent behaviour of polymers are based on the *free-volume* concept. Doolittle and Doolittle [29] introduced this concept in their work on the viscosity of liquids. They assumed that the change in viscosity depends on the distribution of molecule-size holes in the fluid. The sum of these holes represents the *free-volume*, which directly affects the mobility of the liquid molecules. Doolittle and Doolittle [29] expressed this in their semi-empirical expression for the viscosity, η, of liquids:

[2] The excess (configurational) entropy may be defined as the difference between the (configurational) entropy of the polymer above the glass transition temperature and that of the glass in a hypothetical reference state from which, even in principle, no more of the property can be lost due to relaxational processes, Chang et al. [35].

$$\eta = A \exp B \frac{V_\phi}{V_f} = A \exp B \frac{V - V_f}{V_f} = A \exp B \left[\frac{1}{f} - 1 \right]. \qquad \ldots\ldots\ldots (3)$$

Here, A and B are empirical material constants, V_ϕ is the *occupied volume* (i.e., the volume occupied by the molecules of the liquid), and V_f is the *free volume*. This is the unoccupied intermolecular space available for molecular motion. It can also be viewed as the 'excess' volume, i.e., the volume that *exceeds* the occupied volume. Hence, the total macroscopic volume is $V = V_\phi + V_f$, and $f = V_f / V$ called the *fractional free volume*. Figure 4 illustrates these concepts schematically. Although these concepts cannot be formulated rigorously, they make intuitive sense. Temperature affects the free volume. In equation (3), η and f represent the viscosity and the fractional free volume at a given temperature, T. Letting η_0, and f_0 be the same quantities at a conveniently chosen reference temperature, T_0, leads to the *viscosity ratio*:

$$\frac{\eta}{\eta_0} = \exp B \left[\frac{1}{f} - \frac{1}{f_0} \right]. \qquad \ldots\ldots\ldots (4)$$

The Doolittle equation originally referred to liquids consisting of small molecules. Williams et al. [30] adapted it for use with polymers by modifying the Rouse theory of the behaviour of polymers in infinitely dilute solution to the behaviour of polymers in bulk, Ferry [31], p. 225. On the basis of this approach they let:

$$\frac{\eta_f(T)}{\eta_f(T_0)} = \frac{\tau_i(T)}{\tau_i(T_0)} \quad \text{or} \quad \frac{\eta_f}{\eta_{f_0}} = \frac{\tau_i}{\tau_{i0}}, \qquad \ldots\ldots\ldots (5)$$

where η_f is the steady-state viscosity and τ_i is any relaxation time at the same

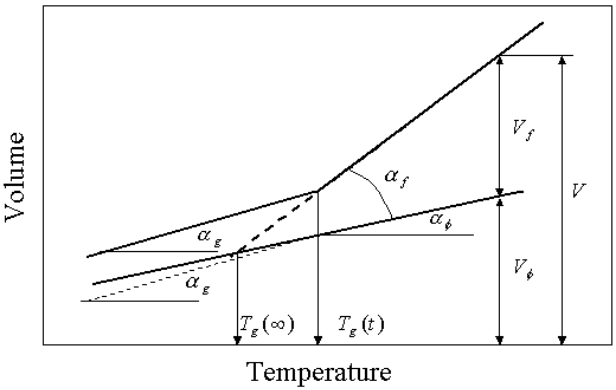

Figure 4: Volume-temperature diagram of an amorphous polymer.

temperature, T . Further, η_{f_0} and τ_{i0} are the same quantities at the reference temperature, T_0. Making use of this proportionality, one may define a *temperature shift factor*, a_T , as an abbreviation for the *temperature shift function*, $a_{T_0}(T)$, to yield:

$$a_T = \frac{\tau}{\tau_0} = \exp B\left[\frac{1}{f} - \frac{1}{f_0}\right]. \qquad \text{…….(6)}$$

If another temperature, say, the glass transition temperature, T_g , is chosen as the reference temperature, we have:

$$a_T = \frac{\tau}{\tau_g} = \exp B\left[\frac{1}{f} - \frac{1}{f_g}\right], \qquad \text{…….(7)}$$

where f_g is the fractional free volume at T_g .

In logarithmic form equation (6) becomes:

$$\log a_T = \frac{B}{2.303}\left[\frac{1}{f(T)} - \frac{1}{f(T_0)}\right] = \frac{B}{2.303}\left[\frac{1}{f} - \frac{1}{f_0}\right], \qquad \text{……. (8)}$$

where $\log a_T$ is the distance required to bring (shift) data recorded at the temperature, T , into superposition with data recorded at the reference temperature, T_0 , along the logarithmic time axis (cf. figure 1). Equation (8) is the starting point for the temperature shift functions that are based on the free volume concept. In sections 3 and 4 we will show that equations of the same form can serve to model the effect of pressure, and that of both pressure *and* temperature.

2.2 The Williams-Landel-Ferry (WLF) model.

Williams et al. [30] modelled the effect of temperature on the mechanical properties of amorphous homopolymers or random copolymers by considering that the fractional free volume of such polymers increases linearly with temperature. They thus let:

$$f = f_0 + \alpha_f (T - T_0), \qquad \text{……. (9)}$$

where α_f is the expansivity (i.e., the isobaric cubic thermal expansion coefficient) of the fractional free volume (cf. figure 4). Substitution of equation (9) into equation (8) leads to:

$$\log a_T = -\frac{(B/2.303 f_0)(T - T_0)}{f_0/\alpha_f + T - T_0} \ . \qquad \text{…….(10)}$$

This is usually used in the form:

$$\log a_T = -\frac{c_1^0 (T - T_0)}{c_2^0 + T - T_0}, \qquad \text{……. (11)}$$

where:

$$c_1^0 = B/2.303 f_0 \qquad \text{..... (12)}$$

and

$$c_2^0 = f_0/\alpha_f \,. \qquad \text{..... (13)}$$

Equation (11) is the *WLF equation*. The superscript ^{0} refers the parameters of the equation to the reference temperature, T_0. If a different reference temperature, say, T_r, is chosen, the constants must be changed using the symmetric relations:

$$c_2^r = c_2^0 + T_r - T_0, \qquad \text{..... (14)}$$

and

$$c_1^r c_2^r = c_1^0 c_2^0 \,. \qquad \text{..... (15)}$$

The product, $c_1 c_2$, is independent of the reference temperature and may therefore be written without superscripts. Referred to the glass transition temperature, the WLF equation becomes:

$$\log a_T = -\frac{c_1^g (T - T_g)}{c_2^g + T - T_g}, \qquad \text{..... (16)}$$

where now, however:

$$c_1^g = B/2.303 f_g \qquad \text{..... (17)}$$

and

$$c_2^g = f_g/\alpha_f, \qquad \text{..... (18)}$$

with f_g as the fractional free volume at the glass transition temperature.

The constants, c_1 and c_2, are found experimentally by *shifting* isothermal segments of the response function into superposition along the logarithmic abscissa to yield a 'master curve' as illustrated in figure 1a. Figure 1b shows master curves at the reference temperature, T_0, and at the experimental temperature, T. The constants are found from the slope and the intercept of a straight line through a plot of $\Delta T/\log a_T$ vs. ΔT, Ferry [31], p. 274. The numerical procedure for calculating the constants is presented in the Appendix A.

Williams et al. [30] also proposed a 'universal' form of the WLF equation having a single adjustable parameter, T_S. This form:

$$\log a_T = -\frac{8.86(T - T_g)}{101.6 + T - T_g}, \qquad \text{..... (19)}$$

has been found not to be truly 'universal' even though it applies reasonably well to many polymeric materials, see, e.g., Schwarzl and Zahradnik [32]. It should therefore be used only as a last resort when the constants, c_1 and c_2, are not available.

It is of interest to obtain the molecular parameters contained in equations (12) and (13). However, there are only two known empirical parameters, the shift constants, c_1 and c_2, available for the determination of the three unknown parameters, B, f_0, and α_f. The most common way to deal with this problem has been to assume that the proportionality factor *B* is unity, Ferry [31], p. 287. In section 4.3 we adduce evidence that this assumption cannot be upheld and show how *B* can be determined experimentally.

2.3 Bueche's temperature (BT) model.

Bueche [33] proposed a 'hole' theory of the free volume that he considered to be a modified form of the WLF equation. He derived:

$$\log a_T = b_1\left[1-\frac{1}{\left[1+b_2(T-T_l)\right]^2}\right], \qquad \text{..... (20)}$$

where

$$b_1 = \frac{9(v^*/v_{fL})^2}{2.303\pi}, \qquad \text{..... (21)}$$

and

$$b_2 = \frac{\alpha_P m}{\rho v_{fL}}. \qquad \text{..... (22)}$$

In these equations, v^* is the critical hole volume for molecular rearrangements, v_{fL} is the free volume per molecular segment at T_L, the threshold temperature (see sections 2.5 and 2.7), α_P is the thermal expansion coefficient, m is the molecular weight of the segment, and ρ is the density. Some of these parameters are not easily determined.

On the strength of the scanty data available to him then, Bueche concluded that his equation provided a better approximation at low temperatures while the WLF equation gave better agreement at higher temperatures. The equation does not seem to have found many users.

2.4 The Bestul-Chang (BC) model.

Bestul and Chang [34], and Chang et al. [35], modelled the effect of temperature by considering the (excess) configurational entropy rather than the free volume. Their logarithmic shift factor takes the form:

$$\log a_T = \frac{B_{BC}}{2.303}\left[\frac{1}{S_c(T)} - \frac{1}{S_c(T_g)}\right], \qquad \text{..... (23)}$$

[cf. equation (8)], where $S_c(T)$ and $S_c(T_g)$ are the excess entropy of the polymer above the glass transition temperature, and that of the glass, respectively. Inserting:

$$S_c(T) = S_c(T_g) + \Delta C_P \int_{T_g}^{T} d\ln T = S_c(T_g) + \Delta C_P \ln(T/T_g), \qquad \text{..... (24)}$$

where ΔC_P is the difference in the specific heats of the polymer in the rubbery or plateau region, and the glassy region, respectively, yields:

$$\log a_T = -\frac{[B_{BC}/2.303\, S_c(T_g)]\ln(T/T_g)}{S_c(T_g)/\Delta C_P + \ln(T/T_g)}. \qquad \text{..... (25)}$$

Since for values near unity $\ln x \approx x-1$, the authors let $\ln(T/T_g) = (T-T_g)/T_g$. This leads to an equation of the form of the WLF equation, where now, however,

$$c_1^g = \frac{B_{BC}}{2.303\, S_c(T_g)}, \qquad \text{..... (26)}$$

and

$$c_2^g = \frac{T_g S_c(T_g)}{\Delta C_P}. \qquad \text{..... (27)}$$

When the experimental temperature, T, is significantly larger than T_g, the approximation used to obtain an equation of the form of the WLF equation may not be adequate. In that case, however, the logarithm may be expanded to any degree desired, using:

$$\ln x = (x-1) - \frac{1}{2}(x-1)^2 + \frac{1}{3}(x-1)^3 - \cdots, \quad 0 < x \le 2, \qquad \text{..... (28)}$$

as long as $T/T_g \le 2$.

2.5 The Goldstein (GS) model.

Goldstein [36] considered excess enthalpy instead of excess entropy. His model may be derived in analogy to the BC model by letting the logarithmic shift factor be given by:

$$\log a_T = \frac{B_{GS}}{2.303}\left(\frac{1}{H(T)} - \frac{1}{H(T_g)}\right), \qquad \text{..... (29)}$$

where $H(T)$ and $H(T_g)$ are the excess enthalpy of the polymer above the glass transition temperature, and that of the glass, respectively. This again leads to a model of the temperature shift factor that is identical in form with that of the WLF model except that now:

$$c_1^g = \frac{B_{GS}}{2.303\,H(T_g)}, \qquad \text{..... (30)}$$

and

$$c_2^g = \frac{H(T_g)}{\Delta C_P}. \qquad \text{..... (31)}$$

2.6 The Adam-Gibbs (AG) model.

Goldstein [36] objected to the use of the entropy alone (as in the BC model) instead of its product with temperature as the principle variable governing glass formation. The model of Adam and Gibbs [37] is free of this objection. They let:

$$\log a_T = -\frac{B_{AG}}{2.303}\left(\frac{1}{TS_c(T)} - \frac{1}{T_r S_c(T_r)}\right), \qquad \text{..... (32)}$$

where

$$S_c(T) = S_c(T_r) + \Delta C_P \ln T/T_r\ , \qquad \text{..... (33)}$$

is the configurational entropy at the temperature, T, and T_r is the reference temperature [cf. equations (24) and (8)]. ΔC_P is the difference in specific heat between the equilibrium melt and the glass that is considered to be independent of the temperature. According to DiMarzio and Gibbs [18, 21, 22], although at higher temperatures the polymer chains are able to assume a large number of configurations, at their second-order thermodynamic transition temperature, T_2, there is only one (or at most a very few) configurations available to the backbone. T_2 is thus the *threshold temperature* below which the relaxation or retardation processes cannot be activated thermally. We therefore assign to it the symbol T_L, taking the subscript L from the Latin *limen*, a threshold. The configurational entropy of the glass is thus deemed to vanish at $T = T_L$. Setting $S_c(T_L) = 0$, equation (33) yields:

$$S_c(T_r) = \Delta C_P \ln T_r/T_L\ . \qquad \text{.....(34)}$$

Substituting this into equation (33) gives $S_c(T) = \Delta C_P \ln T/T_L$ and equation (32) thus again leads to an equation of the form of the WLF equation, with:

$$c_1^r = \frac{B_{AG}}{2.303\Delta C_P T_r \ln(T_r/T_L)}, \qquad \text{..... (35)}$$

and

$$c_2^r = \frac{T_r \ln(T_r/T_L)}{\ln(T_r/T_L) + \left[1 + T_r/(T - T_r)\right]\ln(T_r/T_L)}\ . \qquad \text{..... (36)}$$

The second parameter is a weak function of the temperature, T, involving the reference temperature, T_r, as well as the threshold temperature, T_L. With good approximation:

$$\left[1+T_r/(T-T_r)\right]\ln(T_r/T_L) \approx 1, \qquad \text{..... (37)}$$

and thus:

$$c_2^r \approx \frac{T_r \ln(T_r/T_L)}{1+\ln(T_r/T_L)} \approx T_r - T_L. \qquad \text{..... (38)}$$

The second of these equations again follows upon letting $\ln x \approx x-1$.

2.7 The rate process (RP) model.

A temperature shift factor identical in form with a_T of the WLF equation may be derived also from a modification of the Arrhenius equation well known from the theory of chemical reaction rates. Relaxation (or retardation) may be regarded as a physical process in which the material is carried from state A into state B. The *response time* (relaxation or retardation time) is the time constant for this process. An increase in temperature shortens the response time because it causes the stress to relax, or the strain to reach its ultimate value, faster than at a lower temperature. Consequently, the response time is the reciprocal of the rate at which the physical change takes place, and is thus akin to the reciprocal of a chemical reaction rate. Provided that the conventional theory of reaction rates, Kauzmann [38], is applicable to relaxation and retardation phenomena, one would expect the temperature dependence of these processes, in analogy to that of a chemical reaction, to be given by the equation:

$$\tau = A\exp\frac{\Delta g_a}{\mathbf{R}T}, \qquad \text{..... (39)}$$

where Δg_a is the change in the (molar) free enthalpy[3] of activation for the process per degree of temperature, and **R** is the universal gas constant. The pre-exponential factor *A* is considered to be a constant since it is at most a weak function of temperature.

Equation (39) is the physical equivalent of the Arrhenius equation. According to this equation the relaxation time becomes infinite at the absolute temperature $T=0$. However, an infinite relaxation time implies that the material does *not* relax. For polymers, relaxation or retardation behaviour can become effectively impossible well above $T=0$. The backbone motion, i.e., the main chain segmental motion that gives rise to the response time distribution, ceases below the glass transition temperature,

[3] The free enthalpy (cf. Tschoegl [18], p. 56) is also called the Gibbs free energy or Gibbs potential.

T_g. When this is measured at the usual experimental cooling rate of 5 to 15°C/min, it is about 50°C above T_2. We may therefore set:

$$T_g \approx T_L + 50 . \qquad \text{..... (40)}$$

Subtracting T_L from T modifies equation (39) to allow the response time to become infinite when $T = T_L$. We then have:

$$\tau = A \exp \frac{\Delta g_a}{\mathbf{R}(T - T_L)} . \qquad \text{..... (41)}$$

Model	c_1^g	c_2^g
WLF	$c_1^g = B/2.303 f_g$	$c_2^g = f_g/\alpha_f$
Bestul-Chang	$c_1^g = B_{BC}/2.303 S_c(T_g)$	$c_2^g = T_g S_c(T_g)/\Delta C_P$
Goldstein	$c_1^g = B_{GS}/2.303 H(T_g)$	$c_2^g = H(T_g)/\Delta C_P$
Adams-Gibbs	$c_1^g = B_{AG}/2.303 \Delta C_P T_g \ln(T_g/T_L)$	$c_2^g = T_g - T_L$
Rate Process	$c_1^g = \Delta g_a/2.303 \mathbf{R} c_2^g$	$c_2^g = T_g - T_L$

Table 1: Comparison of the parameters of the temperature superposition models.

Writing equation (41) for τ_0, dividing it into equation (40), and taking logarithms leads to:

$$\log a_T = \frac{\Delta g_a}{2.303\mathbf{R}} \left(\frac{1}{T - T_L} - \frac{1}{T_0 - T_L} \right) . \qquad \text{..... (42)}$$

This may be rearranged to yield equation (11) where now, however,

$$c_1^0 = \frac{\Delta g_a}{2.303 \mathbf{R} c_2^0} , \qquad \text{..... (43)}$$

and

$$c_2^0 = T_0 - T_L . \qquad \text{..... (44)}$$

The former yields an estimate of the apparent molar free enthalpy of activation, while the latter yields one of T_L. Moreover, a plot of $\log a_T$ vs. $1/(c_2^0 + T - T_0)$ yields a straight line with constant slope:

$$\Delta g_a = 2.303\mathbf{R}c_1c_2\,, \qquad \text{..... (45)}$$

as long as these interpretations of the constants c_1^0 and c_2^0 are accepted.

2.8 Critique of the time-temperature superposition models.

Except for Bueche's Temperature (BT) model, all other time-temperature superposition models have the form of the WLF equation or can be reduced to it. They differ only in the interpretation of the parameters of the equation. The Williams-Landel-Ferry (WLF), the Bestul-Chang (BC), the Adam-Gibbs (AG), and the Goldstein (GS) models form a group in that all four consider 'excess' quantities. The rate process (RP) model is, strictly speaking, not based on an excess property although one might consider $T - T_L$ [cf. equation (41)] as the excess of the experimental temperature, T, over the hypothetical reference temperature, T_L.

The BC and AG models are concerned with changes in the configurational entropy. The coincidence between the WLF and BC and AG models becomes understandable if one considers that changes in the configurational entropy arisefrom cooperatively rearranging regions that require free volume in which to move. At constant pressure the change in enthalpy is given by $dH = dU + PdV$, where U is the internal energy. Thus a change in volume underlies also the GS model. Excess (free) volume, excess entropy, and excess enthalpy are fundamentally related, Eisenberg and Saito [39], Shen and Eisenberg [16], and Hutchinson and Kovacs [40]. Theoretically, the excess entropy is an appealing concept. However, volume is much more easily measured experimentally than entropy or enthalpy, and is plausibly related to molecular mobility in a simple manner, Ferry [31], p. 285. We note that the WLF model is the only one that depends on *three* unknown 'molecular' parameters. Since ΔC_P can be determined calorimetrically, all others sport only *two*.

It would clearly be of interest to decide which of the models is the 'correct' one. To do this, one would need to determine separately the molecular parameters in terms of which the models interpret the constants, c_1 and c_2 (see table 1). Unfortunately, only some of those parameters are accessible independently. To see, nevertheless, how one might distinguish between the models based on the free volume, the excess entropy, and the excess enthalpy concepts, we first recall that:

$$\alpha_f = \alpha_e - \alpha_\phi \;\square\; \alpha_q - \alpha_g = \Delta\alpha\,, \qquad \text{..... (46)}$$

and that:

$$\kappa_f = \kappa_e - \kappa_\phi \;\square\; \kappa_q - \kappa_g = \Delta\kappa\,, \qquad \text{..... (47)}$$

where the subscripts *f*, *e*, *q*, and *g* refer to the expansivities and the compressibilities of the free, entire (total), (pseudo-)equilibrium, and glassy volumes, respectively (cf. figure 4). In the second of these equations we have substituted the (pseudo)-equilibrium values for those of the entire volume, and the glassy values for those of the occupied volume. For a justification of the latter, see Moonan and Tschoegl [41].

The change of the free (excess) volume as a function of both temperature and

pressure is given by:

$$dV_{ex} = \frac{\partial V_{ex}}{\partial T} dT + \frac{\partial V_{ex}}{\partial P} dP = V \Delta\alpha dT - V \Delta\kappa dP . \quad \text{..... (48)}$$

Assuming, following Goldstein [36], to whom this treatment is due, that – in the absence of pressure changes – the free volume is constant, i.e., $dV_{ex} = 0$ at and below the glass transition temperature, we have:

$$\frac{dT_g}{dP} = \frac{\Delta\kappa}{\Delta\alpha}, \quad \text{..... (49)}$$

if V_{ex} determines T_g.

For the excess entropy change we have:

$$dS_{ex} = \frac{\partial S_{ex}}{\partial T} dT + \frac{\partial S_{ex}}{\partial P} dP = \left(\frac{\Delta C_P}{T} - \frac{\Delta\alpha^2}{\Delta\kappa} \right) dT , \quad \text{..... (50)}$$

because:

$$\frac{\partial S_{ex}}{\partial T} dT = \frac{\Delta C_P}{T} dT , \quad \text{..... (51)}$$

and

$$\frac{\partial S_{ex}}{\partial P} dP = -\Delta\alpha V dP . \quad \text{..... (52)}$$

But, if we further assume with Goldstein [36] that $dV_{ex} = 0$ implies $dS_{ex} = 0$, then:

$$\frac{dT_g}{dP} = \frac{TV\Delta\alpha}{\Delta C_P}, \quad \text{..... (53)}$$

if it is S_{ex} that determines T_g. Goldstein then shows on the basis of a slightly more involved derivation, that consideration of H_{ex} as the determining factor of T_g also leads to equation (53).

Thus, measurements of dT_g/dP, the change of the glass transition temperature with pressure, combined with determinations of $\Delta\alpha$, $\Delta\kappa$, and ΔC_P should allow one to decide whether it is the free volume on the one hand, or the excess entropy or excess enthalpy on the other hand, that are 'frozen in' at and below the glass transition temperature. So far, measurements have not been made with sufficient accuracy on the same material in the same laboratory to decide the issue unambiguously. Should a valid comparison of equations (49) and (53) have decided against the volume as the governing factor, the question whether it is the excess entropy or the excess enthalpy that determines the glass transition temperature would still appear to be moot. We remark that the hypothetical reference temperature of an excess property is property T_L, not T_g. The Adam–Gibbs (AG) and the Rate Process (RP) models correctly refer to T_L.

2.9 Measurements as functions of temperature.

Hitherto we have considered *isothermal* measurements as a function of time, or of frequency. Measurements are, however, frequently made *isochronically*, i.e., at fixed times or at fixed frequencies. Determinations with the forced-oscillation torsion pendulum are a point in case. The time required to make the measurements must be short compared with the rate at which the temperature is changed. In practice it is changed incrementally and the measurements are taken when thermal and mechanical equilibrium has been reached after each increment. Figure 5 shows a schematic plot of $\log G(T)$ as function of *T*.

The temperature at the inflection point, i.e., the *inflection temperature*, T_{infl}, is sometimes considered to be a rough indication of the glass transition temperature, T_g. A plot of, for instance, the shear modulus, as a function of temperature shows qualitatively the same features as a plot of the same modulus as a function of the logarithmic time. Yet measurements as a function of temperature at a fixed time or frequency cannot be brought into superposition by shifting along the *T*-axis. While the time shift factor, a_T, and hence also its logarithm, is independent of time or frequency [cf. equation (11)], the temperature shift factor, $\Delta T = T - T'$, is evidently a function of the temperature.

A typical set of $G(T)$ vs. *T* curves, for NR (natural rubber), at four isochronal times $t_1 < t_2 < t_3 < t_4$ is shown in figure 6, taken from Prodan [42].

The shorter the time (or the higher the frequency), the slower is the rate of response to an increase in temperature. The slope of the $\log G(T)$ vs. T curve therefore depends both on the steepness of $G(T)$ and the steepness of a_T at the particular isochronal time, in accordance with:

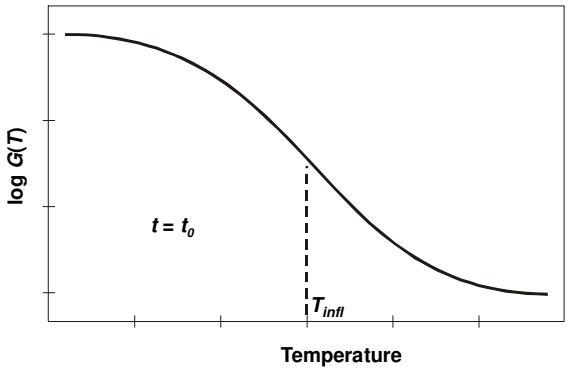

Figure 5: A schematic plot of log *G(T)* vs. *T* .

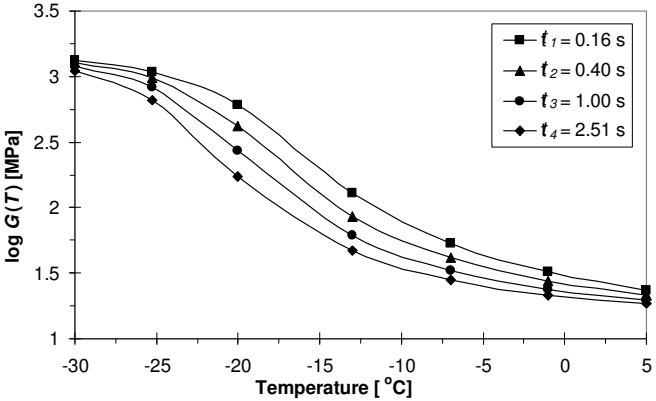

Figure 6: $G(T)$ vs. T for four isochronal times, t_i [42].

$$\left(\frac{\partial \log G(T)}{\partial T}\right)_t = \left(\frac{\partial \log G(T)}{\partial \log t/a_T}\right)_T \left(\frac{\partial \log t/a_T}{\partial T}\right)_t . \qquad \text{..... (54)}$$

Thus, when the temperature response at a fixed time, t, or at a fixed frequency, ω is given, and a_T is known for any reference temperature T_r, the temperature response at any other fixed time t_0, or fixed frequency, ω_0, can be constructed, but this must be done point by point. To do this, we must find the temperature, T', to which the measurement at temperature T must be shifted for a given value of t/t_0 or ω_0/ω.

All this can be understood by the following consideration. Let the parameters of the WLF equation be known for the polymer under investigation. The shift along the T-axis is then given by the relations:

$$\Delta T = \frac{c_2' \log t/t_0}{c_1' - \log t/t_0} = \frac{c_2' \log \omega_0/\omega}{c_1' - \log \omega_0/\omega}, \qquad \text{..... (55)}$$

which are obtained from equation (11) by letting $a_T = t/t_0$, or ω_0/ω, $T - T_0 = \Delta T$, and then solving for ΔT. A modulus measured at the temperature, T, and at the fixed time, t (or the fixed frequency, ω) is therefore equivalent to a modulus measured at the temperature, $T + \Delta T$, and at the fixed time, t_0 (or fixed frequency, ω_0). Thus $G(T;t|\omega) = G(T + \Delta T;t|\omega)$. For each value of the modulus there exists, therefore, a translation along the temperature axis. However, the amount of the translation is not constant but varies with T. Equation (55) allows the construction of master curves of the temperature dependence of a given viscoelastic response function when measurements at a given fixed time or frequency do not cover the entire desired range.

3. MODELLING THE EFFECT OF PRESSURE

Contrary to the case of the effect of temperature, very little has been reported on the effect of pressure. Due to the time-dependent nature of polymers, pressure related material properties, such as the bulk modulus, K, are also functions of time and are not constant as is often assumed. Furthermore, while K is the reciprocal of the bulk compliance, B, the time-dependent *bulk relaxation modulus,* $K(t)$, is *not* the reciprocal of the time-dependent *bulk creep compliance*, $B(t)$. The two are linked through the convolution integral:

$$\int_{-\infty}^{t} K(t-u)B(u)d\ln u = t\ , \qquad \text{..... (56)}$$

and are said to be *time reciprocal.*

Research on the mechanical properties of materials under isotropic pressure began in the early nineteen forties. P. W. Bridgman[4] investigated pressure-induced changes in the compressibility, viscosity, and thermal conductivity of metals and nonmetals [43]. First papers on pressure dependence of the glass transition temperature, T_g, appeared in the sixties [27, 33, 44, 46, 47].

The effect of pressure on the relaxation behavior of *piezo-rheologically simple* polymers is analogous to the effect of temperature on that of *thermo-rheologically simple* ones, taking into account that high temperature corresponds to low pressure and vice versa. In contrast to the effect of temperature, data on the effect of pressure on the time-dependent properties of polymeric materials are relatively scant because they are difficult to determine experimentally.

To model the effect of pressure one thus establishes a pressure shift function, $a_{P_0}(P)$, in analogy to the temperature shift function, $a_{T_0}(T)$. Experimentally, $a_{P_0}(P)$ is found by shifting isobaric segments of a given response function into superposition. The feasibility of time-pressure superposition is demonstrated by the experimental data shown in figure 7, taken from Moonan and Tschoegl [6]. The figure – actually an instant of time-temperature-pressure superposition to be discussed in section 4.3 – displays three shear relaxation master curves at different pressures. The curves are similar in shape and can be shifted into superposition along the logarithmic time axis. Thus, knowing only one relaxation curve, say, the one at the reference pressure, e.g., atmospheric pressure, $P_0 = 0.1\text{MPa}$, the other two curves can be predicted if the pressure shift factor, a_P, is known.

We now turn to the discussion of models for the superposition of the effects of time (or frequency) and pressure. With the exception of the BP model (see section 3.2) they can be shown to be based on the equation:

[4] P. W. Bridgman: "General survey of certain results in the field of high-pressure physics", Nobel Lecture, December 11, (1946)

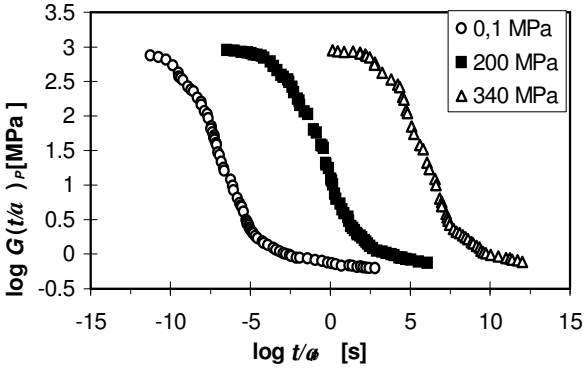

Figure 7: The effect of pressure on the shear modulus, $G(t)$ [6].

$$\log a_P = \frac{B}{2.303}\left[\frac{1}{f(P)} - \frac{1}{f(P_0)}\right] = \frac{B}{2.303}\left[\frac{1}{f} - \frac{1}{f_0}\right], \qquad \text{..... (57)}$$

the pressure analogue of equation (8).

3.1 The Ferry-Stratton (FS) model.

The model proposed by Ferry and Stratton [46] (see also McKinney and Belcher [47], Tribone et al. [48], and Freeman et al. [49]) assumes that the fractional free volume decreases linearly with pressure. Thus:

$$f(P) = f_0 - \kappa_f (P - P_0), \qquad \text{..... (58)}$$

where κ_f is the isothermal compressibility of the fractional free volume, and P is the test pressure while P_0 is the reference pressure at which $f_0 = f(P_0)$ is known. Introducing equation (58) into equation (57) we obtain the Ferry–Stratton equation as:

$$\log a_P = \frac{B}{2.303 f_0}\left[\frac{P - P_0}{f_0 / \kappa_f - (P - P_0)}\right], \qquad \text{..... (59)}$$

or

$$\log a_P = \frac{s_1^0 (P_0 - P)}{s_2^0 + P_0 - P}, \qquad \text{..... (60)}$$

where:

$$s_1^0 = \frac{B}{2.303 f_0}, \qquad \text{..... (61)}$$

and

$$s_2^0 = \frac{f_0}{\kappa_f}. \qquad \text{..... (62)}$$

Equations (60) to (62) are the pressure analogues of the corresponding temperature relations, equations (11) to (13). The equations assume that the temperature is constant and that κ_f does not depend on either T or P.

Equation (60) may be referred to the glass transition pressure, P_g by setting:

$$\log a_P = \frac{s_1^g (P_g - P)}{s_2^g + P_g - P}, \qquad \text{..... (63)}$$

where:

$$s_1^g = \frac{B}{2.303 f_g}, \qquad \text{..... (64)}$$

and

$$s_2^g = \frac{f_g}{\kappa_f}. \qquad \text{..... (65)}$$

These equations were obtained using:

$$s_2^0 + P_0 = s_2^g + P_g, \qquad \text{..... (66)}$$

and

$$s_1^0 s_2^0 = s_1^g s_2^g, \qquad \text{..... (67)}$$

the pressure analogues of equations (14) and (15).

3.2 Bueche's pressure (BP) model.

Bueche [33] proposed a time-pressure superposition model also. His model is not based on equation (57). It gives the logarithmic pressure shift factor as:

$$\log a_P = \frac{P v^*}{2.303 kT}, \qquad \text{..... (68)}$$

where v^* is again the critical hole volume [cf. section 2.3], and k is Boltzmann's constant. Bueche considered his model to be no more than a useful approximation.

3.3 The O'Reilly (OR) model.

O'Reilly [50] derived his model from the observation (Ferry [31], p. 293, Tribone et al. [48], Freeman et al. [49]) that the pressure dependence of the shift factor, a_P, can be described by the simple exponential relation:

$$a_P = \exp\theta(P - P_0), \qquad \ldots\ldots\ldots (69)$$

where $\theta = 1/\Pi f_0$, and Π is a material-dependent empirical parameter that is considered to be independent of the pressure. The model is also referred to as the 'exponential model'. Its logarithmic form becomes:

$$\log a_P = \frac{B}{2.303\Pi f_0}\left(P - P_0\right), \qquad \ldots\ldots\ldots (70)$$

Equating this with equation (57) gives:

$$B\left(\frac{1}{f} - \frac{1}{f_0}\right) = \frac{P - P_0}{\Pi f_0}, \qquad \ldots\ldots\ldots (71)$$

and solving for the fractional free volume, f, yields:

$$f = \frac{\Pi f_0}{\Pi + P - P_0}, \qquad \ldots\ldots\ldots (72)$$

upon setting B equal to 1.

The model supplies the compressibility of the fractional free volume as:

$$\kappa_f = -\left.\frac{\partial f}{\partial P}\right|_T = \frac{f}{\Pi + P - P_0} = \frac{\Pi f_0}{(\Pi + P - P_0)^2}. \qquad \ldots\ldots\ldots (73)$$

In the O'Reilly model, therefore, the fractional free volume, f, depends inversely on the pressure while its compressibility, κ_f, depends inversely on the square of the pressure.

3.4 The Kovacs-Tait (KT) model.

Kovacs and his associates Ramos et al. [52] (see also Tribone et al. [48], and Freeman et al. [49]) proposed a model derived from the compressibility of the Tait equation [53] (see also Fillers and Tschoegl [5]),

$$\kappa_{KT} = -\frac{1}{V_0}\left(\frac{\partial V}{\partial P}\right)_T = \frac{1}{K^*_{KT} + k_{KT}P}. \qquad \ldots\ldots\ldots (74)$$

In thermodynamic equilibrium the compressibility is the reciprocal of the bulk modulus. The subscript 'KT' on the parameters above identifies them as being parameters of the Tait equation. The asterisk signifies that:

$$K^*_{KT}(T) = K_{KT}(T)\big|_{P=P_0}.$$

Equation (74) assumes that the pressure dependence of $K^*_{KT}(T)$ can be accounted for adequately by the first term of a polynomial expansion in the pressure. Integration between the limits V_0, V, and P_0, P, where the subscript 0 denotes the reference state, then leads to:

$$\frac{V-V_0}{V_0} = \ln\left[\frac{K^*_{KT}(T)+k_{KT}P}{K^*_{KT}(T)+k_{KT}P_0}\right]^{-1/k_{KT}}. \qquad \ldots\ldots\ldots (75)$$

The left-hand side of this equation can be expanded to read:

$$\frac{V-V_0}{V_0} = \frac{V_\phi + V_f - V_{0\phi} - V_{0f}}{V_{0\phi} + V_{0f}}. \qquad \ldots\ldots\ldots (76)$$

where V_ϕ, V_f are the occupied and free volumes, respectively [cf. section 2.1], and $V_{0\phi}$, V_{0f} are the same in the reference state. If we now consider that $V_\phi \approx V_{0\phi}$, i.e., that the occupied volume is sensibly the same in the experiment and in the reference conditions, we find that:

$$\frac{V-V_0}{V_0} \approx \frac{V_f}{V_0} - \frac{V_{0f}}{V_0}. \qquad \ldots\ldots\ldots (77)$$

One may now argue that $V_f/V_0 \approx V_f/V = f$ and that $V_{0f}/V_0 = f_0$. The latter appears to be a satisfactory assumption. If the former is accepted also, equation (75) becomes:

$$f - f_0 = \ln\left[\frac{K^*_{KT}(T)+k_{KT}P}{K^*_{KT}(T)+k_{KT}P_0}\right]^{-1/k_{KT}}. \qquad \ldots\ldots\ldots (78)$$

or, equivalently,

$$\frac{f_0-f}{f} = \ln\left[\frac{K^*_{KT}(T)+k_{KT}P}{K^*_{KT}(T)+k_{KT}P_0}\right]^{1/fk_{KT}}. \qquad \ldots\ldots\ldots (79)$$

Equation (78) shows that the fractional free volume of the KT model, just as its compressibility, κ_{KT}, depends inversely on the pressure. Combining equation (57):

$$\ln a_P = \frac{B}{f_0}\left(\frac{f_0-f}{f}\right), \qquad \ldots\ldots\ldots (80)$$

and equation (79) leads to:

$$\log a_P = \frac{B_{KT}}{2.303 f_0}\ln\left[\frac{1+k_{KT}P/K^*_{KT}(T)}{1+k_{KT}P_0/K^*_{KT}(T)}\right]^{1/fk_{KT}}. \qquad \ldots\ldots\ldots (81)$$

Alternatively,

$$\log a_P = \log\left(1+\frac{P-P_0}{C_{KT}}\right)^{\theta_C}, \qquad \ldots\ldots\ldots (82)$$

where $\theta_C = B_{KT}/k_{KT} f_0 f$, and $C_{KT} = K^*_{KT}(T)/k_{KT} + P_0$ is a material-dependent parameter that is a function of the *fixed* experimental temperature, *T*, but is independent of the pressure.

When ΔP is small, we may expand the logarithm according to equation (28) to obtain:

$$\log a_P = \frac{\theta_C}{2.303}\log\left(1+\frac{P-P_0}{C_{KT}}\right) \cong \frac{\theta_C}{2.303}(P-P_0)\,, \qquad \text{..... (83)}$$

and the Kovacs–Tait model reduces thus to that of O'Reilly in form.

3.5 Critique of the time-pressure superposition models.

Table 2 lists the assumptions made by the Ferry–Stratton (FS), the O'Reilly (OR), and the Kovacs–Tait (KT) models for the compressibility of the fractional free volume, κ_f, and for the fractional free volume, f, itself.

We have shown that, leaving Bueche's Pressure (BP) model aside, the timepressure superposition can all be related to equation (57), the pressure analogue of the logarithmic temperature shift factor, equation (8) – and thus to the free volume concept – regardless of the starting point of their derivation. There is, nevertheless, a fundamental difference between time-temperature and time-pressure superposition. While the expansivity of the fractional free volume, does not depend on the temperature above T_g, the compressibility of the fractional free volume, κ_f, must be considered to depend on the pressure below P_g. The differences between the models listed in table 2 thus reside in the assumptions they make about κ_f.

The Ferry–Stratton (FS) model does not make any assumption concerning it. It requires κ_f to be found from equations (61) and (62) just as α_f is to be found from equations (12) and (13). In both cases, however, either parameter can be determined correctly only if *B* is known.

Model	$\log a_P$	κ_f	f
Ferry-Stratton	$\log a_P = \frac{B}{2.303 f_0}\left[\frac{P-P_0}{f_0/\kappa_f - (P-P_0)}\right]$	κ_f	$f = f_0 - \kappa_f (P-P_0)$
O'Reilly	$\log a_P = \frac{B}{2.303\Pi f_0}(P-P_0)$	$\kappa_f = \frac{f}{\Pi + P - P_0}$	$f = \frac{\Pi f_0}{\Pi + P - P_0}$
Kovacs-Tait	$\log a_P = \log\left(1+\frac{P-P_0}{C_{KT}}\right)^{\theta_C}$	$\kappa_{KT} = \frac{1}{K^*_{KT} + k_{KT} P}$	n/a

Table 2: Comparison of models for the time-pressure shift factor, a_P.

Superposition models can be applied successfully only within their range of validity. The pressures encountered in the manufacture of polymeric materials easily exceed 100 *MPa* (Boldizar et al. [54]). A given time-pressure superposition model should therefore yield valid results for pressures at least up to $\approx 100\,MPa$.

The Ferry–Stratton (FS) model achieves satisfactory superposition only for small pressures, usually up to $10\,MPa$. The model is not successful at higher pressures because it does not take into account the pressure dependence of the compressibility. The O'Reilly (OR) and the Kovacs–Tait (KT) models attempt to take this into account. Both models incorporate an inverse dependence of the compressibility on the pressure, albeit in different manner. The OR model predicts a linear dependence of $\log a_P$ on P which is not born out by experiment. The assumption that $V_f / V_0 \gg V_f / V$, inherent in the derivation of the KT model, imposes the restriction that V_0 not be very different from V. Thus, the KT model would seem to be valid only at small pressures. We do not know whether the predictions of the model have ever been tested.

A different approach has been taken by Tschoegl and co-workers [cf. equation (111)]. Their time-temperature-pressure superposition model, called the FMT model for short, will be the subject of section 4.3.

3.6 Measurements as function of pressure.

Measurements can, of course, also be made as function of pressure at a fixed time or frequency, just as they can be made as functions of temperature (cf. figure 6). Again, care must be taken that the material be in thermal and mechanical equilibrium after each pressure increment before the load is applied. A typical set of $G(P)$ vs. P curves, for NR (natural rubber), at four fixed times $t_1 < t_2 < t_3 < t_4$ is shown in figure 8 (taken from Prodan [42]). The curves do not extend much (if at all) beyond the transition regions. It should nevertheless be clear that superposition along the P-axis would not be possible. A point-by-point shifting procedure analogous to that discussed in section 2.9 can, however, be devised again. The shorter the time (or the higher the frequency), the slower is the rate of response to an increase in pressure. The slope of the $\log G(P)$ vs. P curve therefore depends both on the steepness of $G(P)$ and the steepness of a_P at the particular isochronal time, in accordance with:

$$\left(\frac{\partial \log G(P)}{\partial P}\right)_t = \left(\frac{\partial \log G(P)}{\partial \log t/a_P}\right)_P \left(\frac{\partial \log t/a_P}{\partial P}\right)_t . \qquad \text{..... (84)}$$

Thus, when the pressure response at a fixed time, t (or at a fixed frequency, ω), is given, and a_P is known for any reference pressure P_r, the pressure response at any other fixed time, t_0, or fixed frequency, ω_0, can be constructed, but this must be done point by point. To do this, we must find the pressure, P', to which the measurement at the pressure, P, must be shifted for a given value of t/t_0 or ω_0/ω.

In analogy to what has been said about T_{inf}, the inflection temperature, in a plot of $G(P)$ against P the pressure at the inflection point, i.e., the *inflection pressure*, $P_{\text{inf}\,l}$, see Paterson [26], may point to the glass transition pressure, P_g.

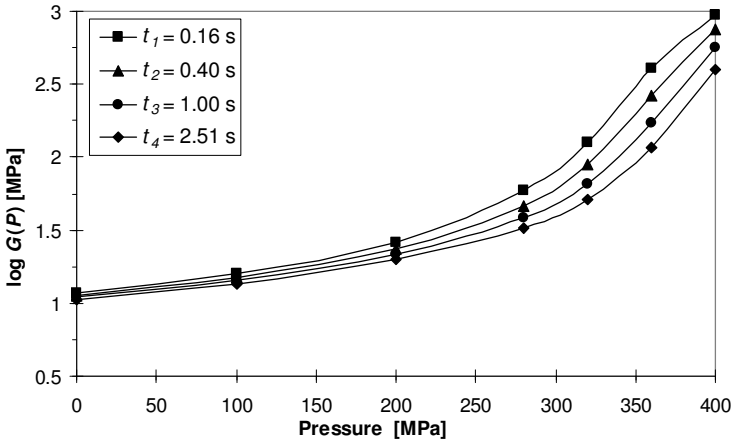

Figure 8: $G(P)$ vs. P for four isochronal times, t_i [6].

4. MODELLING THE EFFECT OF TEMPERATURE *AND* PRESSURE

The preceding section was concerned with time-pressure superposition models. We now turn to time-temperature-pressure superposition models. These are concerned with establishing shift factors $a_{T,P} = a_{T_0,P_0}(T,P)$ that accommodate simultaneously both temperature and pressure changes, and are thus applicable to materials that are both thermo-rheologically *and* piezo-rheologically simple.

4.1 The Simha-Somcynsky (SS) model.

Somcynsky and Simha [55, 56, 57] proposed a hole theory of the liquid state that defines the state in terms of occupied and vacant molecular lattice sites. There are two simultaneous equations to be obeyed. These are:

$$\tilde{P}\tilde{V}/\tilde{T} = \left[1 - 2^{-1/6}\, y(y\tilde{V})^{-1/3}\right]^{-1} + (2y/\tilde{T})(y\tilde{V})^{-2}\left[1{,}011(y\tilde{V})^{-2} - 1{,}2045\right], \quad \text{..... (85)}$$

and

$$y^{-1}\ln(1-y) = (y/6\tilde{T})(y\tilde{V})^{-2}[2.409 - 3033(y\tilde{V})^{-2}] + [2^{-1/6y}(y\tilde{V})^{-1/3} - 1/3][1 - 2^{-1/6}\, y(y\tilde{V})^{-1/3}]^{-1}, \quad \text{..... (86)}$$

where $\tilde{P} = P/P^{\otimes}$, $\tilde{V} = V/V^{\otimes} = v/v^{\otimes}$, and $\tilde{T} = T/T^{\otimes}$ are reduced variables defined in terms of the characteristic values labelled with the superscript $\otimes$. In these equations

y denotes the fraction of occupied lattice sites. If we identify the fraction of empty lattice sites with the fractional free volume, f , we may set, Curro et al. [58]

$$f = 1 - y . \qquad \text{..... (87)}$$

Equations (8) and (59) then give:

$$\log a_{T,P} = \frac{B_{SS}}{2.303}\left(\frac{1}{1-y_0} - \frac{1}{1-y}\right), \qquad \text{..... (88)}$$

where y_0 is the fraction of unoccupied sites under reference conditions. Equation (88) may be called the Simha–Somcynsky (SS) model.

Moonan and Tschoegl [6] modified this equation in light of suggestions by Utracki [59, 60]. The reader is referred to the original papers for details.

4.2 The Havlìček-Ilvalský-Hrouz (HIH) model.

Havlìček et al. [45] extended the Adam–Gibbs theory to account for the effect of pressure. The HIH model expresses $\ln a_{T,P}$ as:

$$\log a_{T,P} = -\frac{B_{HIH}}{2.303}\left(\frac{1}{TS_c(T,P)} - \frac{1}{T_g S_c(T_g,P_g)}\right), \qquad \text{..... (89)}$$

where

$$S_c(T,P) = T\left[\Delta C_P \ln(T/T_L) - V_0(\Delta\alpha P - \vartheta P^2/2)\right], \qquad \text{..... (90)}$$

is the (excess) configurational entropy at the temperature, T , and the pressure, P . T_r and P_r are the reference temperature and pressure, respectively. ΔC_P is again the difference in specific heats between the equilibrium melt and the glass at T_g and P_g , the latter being taken at $0.1MPa \approx 0MPa$. Its temperature dependence is neglected. $\Delta\alpha$ is the change in the coefficient of thermal expansion at atmospheric pressure, and ϑ is a proportionality constant. The pressure dependence of the volume, V , is considered negligible. We could now obtain the prediction of the HIH model for $\log a_{T,P}$ by substituting equation (90) into equation (89) while letting $S_c(T_g,P_g) = 0$, since the entropy of the glass is deemed to vanish. The resulting expression must again undergo certain simplifications to reduce it to the form of the WLF equation. The authors have not done so, probably because the expressions for c_1 and c_2 are rather cumbersome. For $P = 0$ the equations reduce to those of the Adam and Gibbs (AG) model. The equations for dealing with pressure dependence at constant temperature may be found in the paper by Moonan and Tschoegl [6] who also found that the authors had used an inappropriate assumption concerning the pressure dependence of the expansivity, and offered a better form of the temperature dependence.

4.3 The Fillers-Moonan-Tschoegl (FMT) model.

The FMT model (Fillers and Tschoegl [5], Moonan and Tschoegl [6]) can be viewed as an extension of the WLF equation to account for the effect of pressure in addition to that of temperature. Fillers and Tschoegl (see the Appendix for errors in the original publication) take the fractional free volume to depend on both temperature *and* pressure, and therefore write it as:

$$f = f_0 + f_P(T) - f_{T_0}(P)\,. \qquad \ldots\ldots\ldots (91)$$

An alternative derivation may be based on:

$$f = f_0 + f_{P_0}(T) - f_T(P)\,. \qquad \ldots\ldots\ldots (92)$$

Although there is no difference in principle between the two approaches, the former is slightly preferable since it requires knowledge of the pressure dependence of the expansivity while the latter requires knowledge of the temperature dependence of the compressibility, Fillers and Tschoegl [5], that is more difficult to determine. Substitution of equation (91) into equation (8) yields:

$$\log a_{T,P} = -\frac{B}{2.303 f_0}\left[\frac{f_P(T) - f_{T_0}(P)}{f_0 + f_P(T) - f_{T_0}(P)}\right], \qquad \ldots\ldots\ldots (93)$$

as the equation for the time-temperature-pressure superposition shift factor, Fillers and Tschoegl [5, 6]. Now,

$$f_P(T) = \alpha_f(P)[T - T_0], \qquad \ldots\ldots\ldots (94)$$

because the expansivity must be considered to depend on the pressure but its temperature dependence may be neglected as is, indeed, done in deriving the WLF equation. Introducing equation (94) into equation (93) then yields:

$$\log a_{T,P} = -\frac{B}{2.303 f_0}\left[\frac{T - T_0 - \theta(P)}{f_0/\alpha_f(P) + T - T_0 - \theta(P)}\right], \qquad \ldots\ldots\ldots (95)$$

where $\theta(P) = f_{T_0}(P)/\alpha_f(P)$. It remains to find an expression for $f_{T_0}(P)$. If, in analogy to the temperature independence of $\alpha_f(P)$, we assume that the compressibility of the fractional free volume is independent of pressure, we may set:

$$f_{T_0}(P) = \kappa_f(P - P_0)\,, \qquad \ldots\ldots\ldots (96)$$

and, letting $T = T_0$, we regain the Ferry–Stratton model, equation (58). If, on the other hand, we assume that $f_{T_0}(P)$ is inversely proportional to the pressure, we regain the model of O'Reilly (72), by setting:

$$f_{T_0}(P) = \frac{\Pi f_0}{\Pi + P - P_0}\,. \qquad \ldots\ldots\ldots (97)$$

Fillers and Tschoegl [5] also considered the compressibility to depend inversely on the pressure, but their approach differs from that used in the OR and the KT models.

Letting $\kappa_f = \kappa_e - \kappa_\phi$, where κ_e is the compressibility of the entire, and κ_ϕ is that of the occupied volume, they obtained:

$$f_{T_0}(P) = \int_{P_0}^{P} \kappa_T(T_0)dP - \int_{P_0}^{P} \kappa_\phi(T_0)dP . \quad \text{..... (98)}$$

For the first integral they used the compressibility as defined by:

$$\kappa_e = -\frac{1}{V}\left(\frac{\partial V}{\partial P}\right)_T = \frac{1}{K_e^*(T) + k_e P}, \quad \text{..... (99)}$$

where, as in section 3.3 [cf. equation (74)]:

$$K_e^*(T) = K_e(T)\big|_{P=0},$$

is the bulk modulus at zero pressure, and k_e is a proportionality constant deemed independent of either pressure or temperature. In the derivation of the FMT equation its authors further assumed that the pressure dependence of the compressibility of the occupied volume, κ_ϕ, obeys an analogue of equation (99). The integration:

$$f_{T_0}(P) = \int_{P_0}^{P} \frac{1}{K_e^*(T_0) + k_e P} dP - \int_{P_0}^{P} \frac{1}{K_\phi^*(T_0) + k_\phi P} dP , \quad \text{..... (100)}$$

then yields:

$$\log a_{T,P} = -\frac{c_1^{00}[T - T_0 - \theta(P)]}{c_2^{00}(P) + T - T_0 - \theta(P)}, \quad \text{..... (101)}$$

where

$$\theta(P) = c_3^0(P)\ln\left(\frac{1 + c_4^0 P}{1 + c_4^0 P_0}\right) - c_5^0(P)\ln\left(\frac{1 + c_6^0 P}{1 + c_6^0 P_0}\right), \quad \text{..... (102)}$$

and the *c*'s follow as:

$$c_1^{00} = B / 2.303 f_0 , \quad \text{..... (103)}$$

$$c_2^{00} = f_0 / \alpha_f(P), \quad \text{..... (104)}$$

$$c_3^0(P) = 1 / k_e \alpha_f(P), \quad \text{..... (105)}$$

$$c_4^0 = k_e / K_e^*, \quad \text{..... (106)}$$

$$c_5^0(P) = 1 / k_\phi \alpha_f(P), \quad \text{..... (107)}$$

$$c_6^0 = k_\phi \big/ K_\phi^* . \quad \text{..... (108)}$$

The ^{00} superscript indicates that the parameter is referred to the reference temperature T_0 (first place) and to the reference pressure P_0 (second place). A single ^{0} superscript

refers to the reference temperature only. The * superscript refers to zero (in practice, atmospheric) pressure.

Equation (101) is the Fillers–Moonan–Tschoegl or FMT equation. K_ϕ^* and k_e, and thus c_4^0, can be determined from separate volume-pressure measurements through a fit to the equation:

$$\ln\frac{V}{V_0} = -\frac{1}{k_e}\ln\left[\frac{K_e^*(T)+k_eP}{K_e^*(T)+k_eP_0}\right], \qquad \text{..... (109)}$$

by a non-linear least-squares procedure. Equation (109) is known in the form:

$$V = V_0\left[\frac{K_e^*(T)+k_eP}{K_e^*(T)+k_eP_0}\right]^{-1/k_e}, \qquad \text{..... (110)}$$

as the equation of Murnaghan[5] [61]. The latter is obtained by integrating equation (99) at constant temperature between the limits V_0, P_0, and V, P.

In conjunction with c_4^0 the five equations for c_1^0, c_2^0, c_3^0, c_4^0, c_5^0, and c_6^0 are clearly sufficient to uniquely determine B, f_0, α_f, K_ϕ^* and k_ϕ. This strongly suggests that the temperature and/or pressure dependence of polymers be characterized always by carrying out both isothermal and isobaric measurements. The measurements by Fillers and Tschoegl [5], Moonan and Tschoegl [6], Simha and Wilson [56], and the recent ones by Kralj et al. [1], Prodan [42], and Emri at al. [62] indicate that for most polymers B is not equal to 1, as has been assumed for many years. This leads to the conclusion, that many data on f_0 and α_f available today for several polymers may not represent the best estimates.

We note that setting $\theta(P)=0$ (i.e., performing the experiments at the reference pressure), the FMT equation reduces to the WLF equation. On the other hand, executing the experiments at the reference temperature, i.e., setting $T=T_0$, leads to:

$$\log a_P = \frac{B}{2.303f_0}\left[\frac{\theta(P)}{f_0/\alpha_f(P)-\theta(P)}\right] = \frac{c_1^{00}\,\theta(P)}{c_2^{00}(P)-\theta(P)}. \qquad \text{..... (111)}$$

Equation (111) becomes the Ferry–Stratton equation (60), upon the substitutions $\theta(P)\to(P-P_0)$, $c_1^{00}\to s_1^0$, and $c_2^{00}(P)\to s_2^0$. Within its domain of validity the FMT model can therefore handle time-temperature, time-pressure, and time-temperature-pressure superposition equally well.

---

[5] The difference between the Tait and the Murnaghan compressibilities, Equations (74) and (99), is rather similar to that between the 'engineering' or 'nominal' stress, $\sigma = F/A_0$, and the 'true' stress, $\sigma = F/A$, where F is the force, and A is the area upon which the former acts. In both relations the subscript 0 denotes the initial, i.e., undeformed quantity.

4.4 Critique of the time-temperature-pressure superposition models.

Table 3 lists the logarithmic shift factors, $\log a_{T,P}$, of the Simha–Somcynsky (SS), the Havlìček-Ilvalský-Hrouz (HIH), and the Fillers–Moonan–Tschoegl (FMT) models along with the approach on which each model is based.

Model	$\log a_{T,P}$	**Approach**
Simha-Somcynsky	$\log a_{T,P} = \frac{B_{SS}}{2.303}\left(\frac{1}{1-y_0}-\frac{1}{1-y}\right)$	Hole theory
Havlìček-Ilvalský-Hrouz	$\log a_{T,P} = -\frac{B_{HIH}}{2.303}\left(\frac{1}{TS_c(T,P)}-\frac{1}{T_g S_c(T_g,P_g)}\right)$	Excess entropy
Fillers-Moonan-Tschoegl	$\log a_{T,P} = -\frac{B}{2.303 f_0}\left[\frac{T-T_0-\theta(P)}{f_0/\alpha_f(P)+T-T_0-\theta(P)}\right]$	Free volume

Table 3. Comparison of models for the time-temperature-pressure shift factor, $a_{T,P}$.

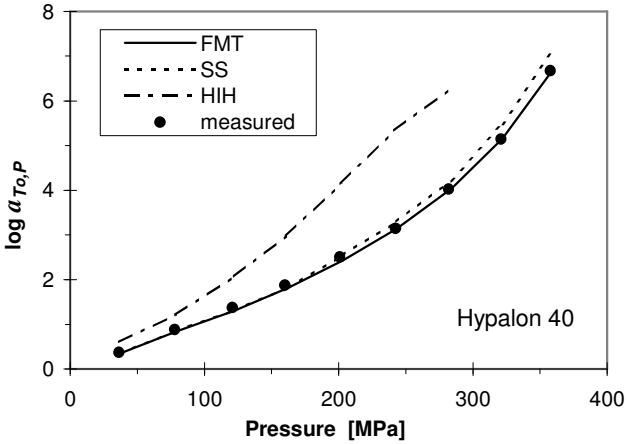

Figure 9: Comparison of $\log a_{T_0,P}$, obtained from the HIH, SS, and FMT models.

The three models differ considerably in their approach and in their usefulness. Moonan and Tschoegl [6] discussed all three in depth. Figure 9, which reproduces part of figure 21 of the paper by Moonan and Tschoegl [6], compares the logarithmic shift factors, $\log a_{T_0,P}$, for Hypalon 40 rubber, that were obtained using the three models.

Clearly, the HIH model is not in agreement with the experimental values while the SS and the FMT models both describe the data about equally well. Moonan and Tschoegl [6] stated that the improved form of the HIH model fits the data as well as the FMT equation, but is certainly not more convenient to use. Furthermore, it is perhaps flawed since it requires knowledge of the change in the heat capacity, ΔC_P, and when this is determined from a fit to the shift data, it does not agree with calorimetric data.

All this, paired with the capability of the FMT model to describe all three types of superposition, appears to make it the model of choice.

4.5 CEM Pressure apparatus.

Recently Kralj et al. [1], and Emri and Prodan [62] reported on the experimental setup for characterization of the effect of pressure and temperature on behavior of solid polymers. The system assembly is shown schematically in figure (10).

The pressure is generated by the *pressurizing system* using silicone oil. The *pressure vessel* is contained within the *thermal bath*, where another silicone oil circulates from the *circulator*, used for precise temperature control. The apparatus utilizes two separate *measuring inserts*, which can be inserted into the pressure vessel: the *dilatometer* and the *relaxometer*. Signals from the measuring inserts pass through

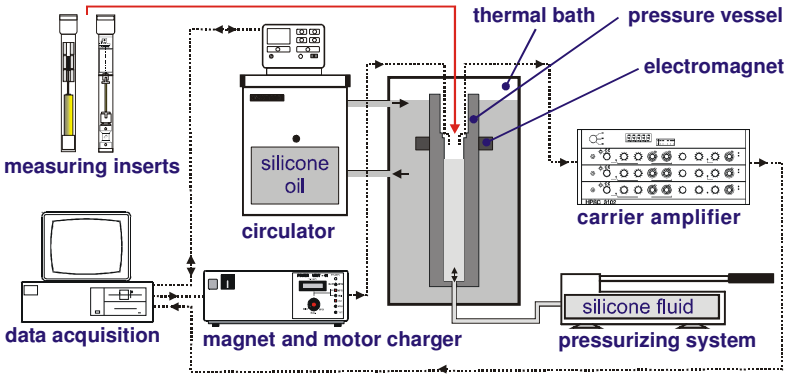

Figure 10. Schematic of the CEM Measuring System [1, 62].

the *carrier amplifier* prior to being collected in digital format by the *data acquisition* system.

The magnet and motor charger supplies current to the *electromagnet*, which activates the measurement. The same charger also supplies current to the *electric motor* of the *relaxometer*, shown in figure 10, which pre-loads the spring that then applies the desired torsional deformation (angular displacement), to the specimen. Specimens can be simultaneously subjected to pressures of up to $500\,MPa$ with a precision of $\pm 0.1\,MPa$, and to temperatures ranging from –50°C to +120°C with a precision of ±0.01°C.

The *dilatometer* measures bulk properties such as the: bulk creep compliance, $B(t,T,P)$; equilibrium bulk creep compliance, $B(T,P)=B(t\to\infty,T,P)$; equilibrium bulk modulus; $K(T,P)=K(t\to\infty,T,P)=1/B(T,P)$; specific volume $v(T,P)=v(t\to\infty,T,P)$, and thermal (equilibrium) expansion coefficient, $\beta(T,P)=\beta(t\to\infty,T,P)$. The measurements are performed by monitoring the volume change of the specimen, which results from the imposed changes in pressure and/or temperature, by measuring the change in length of the specimen, $L(t,T,P)$, with the aid of a built-in Linear Variable Differential Transformer (LVDT). The volume estimate can be considered accurate if the change in volume is small (up to a few percent) and the material is isotropic. Specimens for the *dilatometer* can be up to 16 mm in diameter and from 40 to 60 mm in length. The absolute volume measurement error is about 0.1%, while the relative error is 0.05%.

The *relaxometer* measures the shear relaxation modulus by applying a constant torsional strain to a cylindrical specimen, in which the induced moment is monitored over time. The two main parts of the insert are the *loading device* and the *load cell*. The *loading device* applies a constant torsional strain by twisting the specimen for a few degrees in less than 0.01 seconds. The deformation of the specimen occurs by first pre-loading an Archimedes spring with the *electric motor*. Once twisted, the spring is kept in its pre-loaded position by a pawl-rack mechanism. Then, the *electric magnet*, mounted outside the pressure vessel, pulls the pawl out of the rack, and the energy of the spring deforms the specimen to a pre-determined angle, which can range from 1° to 15°. The induced moment is then measured by the *load cell*, which is attached to the *slider mechanism* to compensate for specimen's length changes, resulting from various temperature and pressure conditions. After the shear relaxation measurement is complete, the *electric motor* brings the specimen to its original undeformed state, while maintaining the pressure vessel fully pressurized. Specimen's diameter can range from 2.5 mm to 12 mm while its length from 50 mm to 58 mm. The *relaxometer* can measure shear moduli ranging from $0.01\,MPa$ to $10.000\,MPa$, with accuracy within $\pm 5\%$ of the initial specimen's modulus value.

The measuring capabilities of the system are summarized in table 4. In the upper part are listed physical quantities that are measurable "directly". These are the shear moment, $M(t,T,P)$, and the specimen length, $L(t,T,P)$, measured as functions of time at selected temperatures and pressures. In the second part of table 4 are listed quantities that may be calculated from "simple definitions". The third part lists quantities that need to be extracted from the WLF and/or FMT model.

	Physical Properties	Symbols
Measured	Shear moment.	$M(t), M(T), M(P)$ or $M(t,T,P)$
	Specimen length.	$L(t), L(T), L(P)$ or $L(t,T,P)$
Calculated from definitions	Shear relaxation modulus.	$G(t), G(T), G(P)$ or $G(t,T,P)$
	Specific volume.	$v(t), v(T), v(P)$ or $v(t,T,P)$
	Linear thermal expansion coefficient.	$\alpha(T), \alpha(P)$ or $\alpha(T,P)$
	Volumetric thermal expansion coefficient.	$\beta(T), \beta(P), \beta_g, \beta_e, \beta_f$ or $\beta_{g,e,f}(T,P)$
	Bulk creep compliance.	$B(t), B(T), B(P)$ or $B(t,T,P)$
	Bulk modulus.	$K(T), K(P)$ or $K(T,P)$
Calculated from models	WLF constants.	c_1, c_2
	WLF material parameters.	α_f, f_0
	FMT constants.	$c_1, c_2, c_3, c_4, c_5, c_6$
	FMT material parameters.	$\alpha_f(P), f_0(P), B, K_e^*, k_e, K_\Phi, k_\Phi$

Table 4: Measuring capabilities of the CEM apparatus.

All together, the system measures five physical quantities: temperature, $T(t)$; pressure, $P(t)$; torsional deformation (angular displacement) per unit length, ϑ_0, applied to the specimen at $t=0$; specimen length $L(t,T,P)$; and the decaying torque, $M(t,T,P)$, resulting from the initial torsional deformation, φ_0. Using these physical quantities, measured at constant or varying temperature and pressure, we can obtain the material properties listed in table 4.

5. SUPERPOSITION IN THE TRANSITION REGION.

There are two features that require comment. The first is the effect of rigid particulate or fibrillar fillers, and – in crosslinked materials – the effect of the crosslink density on time-temperature superposition. There is currently no information on the effect of fillers and of crosslink density on time-pressure superposition. The second is the effect of temperature and pressure not on the time dependence of the mechanical behavior but on the response functions themselves. The effect of temperature may be accounted for by applying *vertical shifts*. No vertical shifts have been suggested as yet for time-pressure superposition.

5.1 Fillers and crosslinks.

Polymeric materials may be filled to varying degrees with a rigid filler that itself shows no appreciable time-temperature-pressure dependence. If the filler itself shows time dependence, the material is a two-phase material and is not thermo-rheologically simple. If the volume fraction, ψ, of a rigid filler is not too large, the filled material generally obeys the WLF equation governing the behavior of the matrix. The parameters of the equation may change, however, if ψ is large enough to affect the mobility of the chains of the matrix polymer. They may also change if the matrix polymer adheres to the filler. In a filled elastomer one distinguishes *reinforcing* fillers, the addition of which enhances rupture strength (e.g., certain types of carbon black,) and *non-reinforcing* fillers (e.g., salts or glass beads). Stacer and Husband [63] found that in systems in which the polymer is weakly adsorbed to a non-reinforcing filler an interface may form that introduces a secondary transition. Application of the WLF equation is then affected by the existence of this secondary transition. If the polymer chains are strongly adsorbed to the particles of a reinforcing filler (as is the case, e.g., with certain types of carbon black) the filler particles can act as (physical) cross links. Duperray and Leblanc [64] found that in elastomers highly filled with carbon black $E'(\omega)$ and $E''(\omega)$ did not superpose with the same parameters of the WLF equation. They also found that in their highly filled systems the distribution of relaxation times did not conform to equation (1).

Elastomers form a three-dimensional network of covalently (chemically) cross-linked polymer chains. In chemically crosslinked systems the density of cross-linking can influence superposability. A high degree of cross linking as is present in, e.g., the phenolics and melamines, may drastically lower chain mobility, and therefore the threshold temperature, turning WLF into something resembling an RP behavior (see section 2.7).

5.2 Vertical shifts.

Successful application of the superposition principles may require certain adjustments (vertical shifts) to the linear viscoelastic responses such as the moduli, compliances, viscosities and fluidities, Ferry [31], chapter 11). The vertical shifts take the form exemplified by:

$$G_p(t) = G(t)\frac{T_0\rho_0}{T\rho}, \qquad \text{..... (112)}$$

and/or

$$J_p(t) = J(t)\frac{T\rho}{T_0\rho_0}, \qquad \text{..... (113)}$$

where the subscript p refers to the vertically shifted response function, and ρ and ρ_0 are the density of the polymer at T and T_0, respectively. The ratio $T\rho/T_0\rho_0$ its reciprocal are referred to as the *vertical shift factors*. The density ratio is often omitted

because – particularly when plotting the response function in logarithmic coordinates – it is deemed negligible.

The blanket application of the vertical shift factors does not appear to be incontrovertible in all cases. The various components of the response functions generally require different adjustments. We first consider the stress-response functions exemplified by the (shear) creep compliance:

$$J(t) = J_g + \int_{-\infty}^{\infty} L(\tau)\left[1-\exp(t/\tau)\right] d\ln\tau + \left\{\phi_f t\right\}. \qquad \text{..... (114)}$$

Here J_g, the glass compliance, represents the purely elastic, the integral over the retardation spectrum, $L(\tau)$ represents the viscoelastic, and $\phi_f t$ represents the purely viscous contribution. In the latter $\phi_f = 1/\eta_f$ is the steady-state fluidity, the reciprocal of the steady-state viscosity. The braces around the last term signify that this term is absent if the material is arrheodictic (i.e., does not show steady-state flow; see Tschoegl [2], p. 93).

The vertical shift factor $T\rho/T_0\rho_0$, being suggested by the flexible chain theory (Ferry 31, chapter 11), is really not applicable to the glass compliance, J_g. Excluding J_g from the vertical shift leads to:

$$J_p(t) = J_g + \left[J(t) - J_g\right]\frac{T\rho}{T_0\rho_0}, \qquad \text{..... (115)}$$

and this equation has indeed found application.

McCrum [65] defined three vertical shift factors, b_T, c_T, and d_T, which he applied to the creep compliance. We follow here McCrum's notation to indicate the temperature dependence of the compliances as superscripts. The coefficient b_T is the ratio of the difference, J_e^T and J_g^T, between the equilibrium and the glassy shear compliance at the temperature, T, to the same difference, $J_e^{T_0}$ and $J_g^{T_0}$, at the reference temperature, T_0. Thus:

$$b_T = \frac{J_e^T - J_g^T}{J_e^{T_0} - J_g^{T_0}}. \qquad \text{..... (116)}$$

The coefficient c_T is given by:

$$c_T = \frac{J_g^T}{J_g^{T_0}}, \qquad \text{..... (117)}$$

and the factor d_T by:

$$d_T = \frac{J_e^T}{J_e^{T_0}}. \qquad \text{..... (118)}$$

McCrum used these vertical shift factors to obtain $J_P^T(t)$ in a procedure that is too involved to be reproduced here in detail. The reader is referred to the original references (McCrum and Morris [65], McCrum et al. [66], and McCrum [67]).

In the strain-response functions exemplified by the (shear) modulus the viscoelastic and the viscous contributions are not separated from one another. The (shear) relaxation modulus is given by:

$$\begin{aligned} G(t) &= \{G_e\} + \int_{-\infty}^{\infty} H(\tau)\exp(t/\tau)\, d\ln\tau \\ &= G_g + \int_{-\infty}^{\infty} H(\tau)\left[1-\exp(t/\tau)\right] d\ln\tau\,, \end{aligned} \qquad \ldots\ldots\ldots (119)$$

where the viscoelastic and the viscous component are combined into a single expression, G_e being the equilibrium, and G_g the glassy modulus, while $H(\tau)$ is the relaxation spectrum. The braces around G_e signify that G_e is absent if the material is rheodictic. On the basis of the second of equations (119) we may argue that the glassy component, G_g, may be separated out from the viscoelastic-viscous component and that we may hence write:

$$G_p(t) = G_g + \left[G(t) - G_g\right]\frac{T_0\rho_0}{T\rho}\,, \qquad \ldots\ldots\ldots (120)$$

in analogy with the case of $J(t)$. We note that [2]:

$$G_e^{\{0\}} J_e^{\{0\}} = 1\,,\quad G_g G_e = 1\,, \text{ and } \eta_f \phi_f = 1\,, \qquad \ldots\ldots\ldots (121)$$

and their relation to the relaxation, $H(\tau)$ and the retardation, $L(\tau)$, spectra:

$$G_g - \{G_e\} = \int_{-\infty}^{\infty} H(\tau) d\ln\tau\,, \qquad \ldots\ldots\ldots (122)$$

$$J_e^{\{0\}} - J_g = \int_{-\infty}^{\infty} L(\tau) d\ln\tau\,, \qquad \ldots\ldots\ldots (123)$$

and

$$\eta_f = \int_{-\infty}^{\infty} \tau H(\tau) d\ln\tau\,. \qquad \ldots\ldots\ldots (124)$$

A different vertical shift procedure was advocated by Rusch [68, 69] who proposed to use T/T_e where T_e is the 'effective' temperature (see section 6.1) for the vertical shift factor but admitted that this suggestion lacks theoretical (physical) foundation.

Although no use of vertical shift factors has hitherto been reported in dealing with time-pressure superposition, the change in density, $\rho(P)/\rho(P_0)$ might evidently be considered.

6. SUPERPOSITION IN THE GLASSY REGION

We have discussed the effect of temperature on the mechanical properties of polymeric materials in the (*main*) *transition region* (cf. figure 3), i.e., in the region between the *glassy* and the *rubbery* or the *plateau* region, in which the response times arise from segmental motions of the backbone chains. Special considerations apply outside this region. In the glassy region, i.e., below T_g, or above P_g, segmental rearrangements of the backbones cannot be detected on the time scale of any experiment executed in an affordable time frame. The material is, however, not in thermodynamic equilibrium and generally undergoes structural changes commonly referred to as *physical aging*. In the presence of physical aging any possible shift function becomes a function of time. Because of the absence of equilibrium these changes are outside the scope of this paper (cf., however, Emri et al. [70]). Nevertheless, two topics concerning time-temperature superposition in the glassy region do need to be mentioned here.

6.1. Applicability of the WLF equation in the glassy region.

In the glassy region any attempt to shift isothermal segments into superposition cannot follow an equation of the WLF type as discussed in section 2.2. All equations of the WLF type predict that $\log a_T$ diverges when $T = T_g - c_2^g$. Thus T must be larger than $T_g + c_2^g$. Indeed, it is found that values of $\log a_T$, determined experimentally by shifting, depart from the prediction of the WLF equation and begin to 'bend over' below the glass transition temperature. This is shown in figure 11 adapted from Schwarzl and Zahradnik [32].

Rusch [68] suggested that time-temperature superposition below T_g at constant pressure be effected using a modified WLF equation that makes use of the 'effective' temperature of Tool [71]. The reader is referred to Rusch's original article for details. In the glassy state polymers are, in principle, always in a non-equilibrium state. The properties of the material depend on the path along which material has entered the glassy state. If materials are far below the glass transition then their properties are time-independent for all practical purposes. However, in the vicinity of the glass transition materials exhibit significant time-dependent changing of all physical properties, known as physical aging. Kovacs [72] was among the first who studied these phenomena. We will refrain from reviewing the phenomena of physical aging because this subject requires a paper on its own.

6.2 Higher-order transitions.

In virtually all polymers there exist below the glass transition temperature so-called *secondary*, *tertiary*, etc., transitions. These β-, γ-, etc., transitions are distinct from the α-, or *main*, transition. While the latter results from the motion of chain segments, the higher-order transitions arise not from main chain segmental motion but, typically, from motion of side chains attached to the main chain, or from crankshaft and kink motions, or other molecular rearrangements (Ferry [31], pp. 450-451). Often

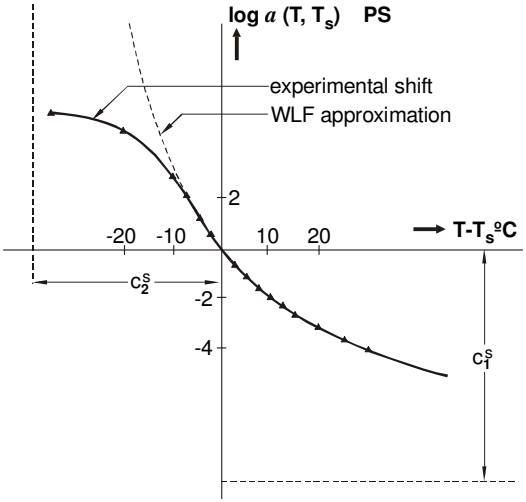

Figure 11: The logarithmic shift factor, $\log a_T$, above and below T_g.

a secondary transition appears to be characterized by a single response time. More generally it, also, exhibits a distribution of response times just as a main transition does, although a secondary transition is usually less broad.

It is sometimes claimed that time-temperature superposition of secondary and higher-order transitions can be effected using the physical equivalent of the Arrhenius equation (38). This assumes the threshold temperature, T_L, for one of these transitions to be the absolute zero of temperature. The applicability of equation (38) to secondary transitions is, however, questionable on theoretical grounds. It is unlikely that these motions should 'freeze in', as it were, at $T = 0$. The molecular motions giving rise to higher transitions also require free volume in which to move. It is more likely, therefore, that these transitions should also obey a relation of the form of equation (40) albeit with a rather low threshold temperature of possibly only a few degrees Kelvin. Equation (40) with such a low T_L would be difficult to distinguish from equation (38). Be that as it may, however, we may expect that advances in the accuracy of determining and reporting linear viscoelastic responses will force a more fundamental look at the presence of secondary transitions in the future. Ferry [31] (page 310), has carefully investigated time-temperature superposition in the β-transition of poly(n-butyl methacrylate). Knauss and Zhu [73] have more recently investigated the β-transition of polycarbonate.

Since superposition does not apply in the presence of more than one viscoelastic mechanism [cf. equation (1)], the question arises whether thermo-rheologically simple materials exist at all. Strictly speaking, neither the WLF nor the FMT equation is valid in cases where the material exhibits higher-order transitions.

However, since the α-transition generally overwhelms the behaviour resulting from the presence of secondary and also higher-order transitions, the influences of the latter have commonly been neglected. This practice is bolstered by the fact that linearly viscoelastic responses are generally reported in logarithmic coordinates that normally mask the relatively small effect of the higher transitions. Also, the presence of secondary transitions may not unduly affect the location or breadth of the α-transition. Certainly, when a polymer may be deemed thermo-rheologically simple, time-temperature superposition affords a welcome means of extending the experimental time scale.

7. SUPERPOSITION IN THE RUBBERY AND PLATEAU REGIONS

Completely different problems may arise in the rubbery and plateau regions and in the terminal or flow region. We only briefly refer here to material characteristics that would influence any superposition scheme in their presence, even though no such schemes have as yet been proposed and their development may, in fact, be illusory. Again, contour plots may furnish the only workable data representation in the presence of some of these characteristics.

7.1 Crystallinity and crosslinking.

If the structure of a polymer chain is sufficiently regular, or if it contains long enough sequences that have a regular structure, the regions of regular structure will 'close-pack', i.e., they will form crystallites, dendrites, or spherulites, structures of increasing complexity [74-79]. The presence of crystalline structures raises the modulus in the plateau region, as illustrated in figure 12.

An increase in the degree of crystallinity, ξ, broadens the plateau region and moves it to shorter times. The dotted line represents the hypothetical case of 100% crystallinity. As observed by Prodan [42] on polyamide (PA6), this effect of crystallinity may appear at lower values of ξ and at shorter times, in creep than in relaxation.

Crystalline regions may interconnect to form superstructures [80]. A *superstructure* is a network of crystalline regions interconnected by chains that leave and enter several of them in sequence. The formation of superstructures is generally enhanced by orientation brought about by, for instance, drawing or rolling. Superstructure increases the value of ξ as revealed most clearly by small angle x-ray, and NMR analysis [81].

A crystalline polymer does not exhibit a well-defined melting point but a melting region whose extend depends primarily on the degree of crystallinity, and the molecular mass (weight) distribution of the crystalline regions. Furthermore, the breadth of the melting regions depends on the rate of heating or cooling applied. In the construction of contour plots for crystalline polymers the thermal history must therefore be carefully stated.

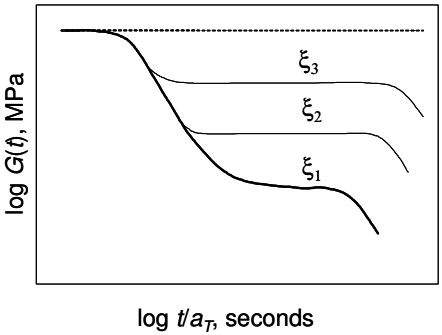

Figure 12: Schematic illustrating the effect of the degree of crystallinity, ξ, on $G(t)$.

7.2 Chemical relaxation.

Accessing the rubbery and plateau regions and the terminal or flow region may require experiments at elevated temperatures. At sufficiently high temperatures there is then the danger of *chemical relaxation*, brought about by chain scission, and possibly recombination. Experiments at higher temperatures should generally be carried out under a protective nitrogen blanket (Tobolsky [82, 83]; Ferry [31], p. 425). Some chemical relaxation may occur at high temperatures even if oxygen is effectively excluded.

8. SUPERPOSITION IN THE TERMINAL OR FLOW REGION

The terminal region of a rheodictic material is characterized by the steady-state, or steady-flow fluidity, ϕ_f, or its reciprocal, the steady-state, or steady-flow viscosity, η_f. A rheodictic (i.e., uncrosslinked) polymer is a *polymer melt*. Polymer melts are non-Newtonian liquids whose steady-state fluidity or viscosity depends on the rate of shear, $\dot{\gamma}$. Measurements of ϕ_f or η_f made at finite rates of shear should therefore be extrapolated to zero shear rate.

Values of η_f measured at different temperatures may be superposed using:

$$a_T = \frac{\eta_f(T)T_0\rho_0}{\eta_f(T_0)T\rho}, \qquad \text{..... (125)}$$

where $\eta_f(T)$ is the steady-state viscosity at the temperature, T, and ρ is the density, while the subscript 0 refers to the reference temperature and density. A plot of the *reduced viscosity*, $\eta_r = \eta(\dot{\gamma})/\eta(\dot{\gamma}_0)$ against $\dot{\gamma}a_T$, results in a single composite curve (Ferry [31], p. 380).

Superstructures (cf. section 7.1) can persist in the flow region and can interfere with superposability. Careful measurements by Plazek [8, 84] have shown that shift factors in the transition and in the terminal zone may be somewhat different. Other observations of this kind are discussed by Ferry 31, pp. 305ff.

Prodan [42] shifted creep and relaxation data on polyamide (PA6), and constructed master curves for both, applying the same pair of WLF constants. However, when the two response curves were interconverted (using the interconversion algorithm described by Tschoegl and Emri [85, 86]), they differed in their behaviour in the flow region. He tentatively ascribed this to interaction of the long-chain components of the molecular mass distribution with the crystalline superstructure.

9. SUPERPOSITION IN DEFORMATIONS OTHER THAN SHEAR.

In small deformation, time- or frequency-dependent changes in *shape* (shear) and changes in *size* (bulk) are neatly separated. The former are expressed by the *shear relaxation* and the *shear storage* and *loss modulus*, as well as the *shear creep* and *shear storage and loss compliance*, while the latter are described by the *bulk relaxation* and *bulk storage* and *loss modulus*, as well as the *bulk creep* and *bulk storage* and *loss compliance*. In this sense the shear and the bulk properties are *fundamental properties*. Response functions that describe simultaneously changes in shape and in size, such as the *tensile relaxation modulus* and *creep compliance*, and the *longitudinal bulk relaxation modulus* and *longitudinal bulk creep compliance*, as well as the corresponding storage and loss functions, are, in this sense, *derived functions*.

The superposition models described in this paper treated superposition in terms of the shear properties. There is compelling evidence for superposability in the tensile properties also. Evidence for the same in the bulk properties has been claimed by McKinney and Belcher [47]. Recent measurements of Deng and Knauss [87] and Sane and Knauss [88] in shear and in bulk on two different specimens of the same PVAc (poly(vinyl acetate)) sample appear to support this contention. A definite proof would require measurements in shear and in bulk that were carried out in accordance with the *Standard Protocol* proposed by Tschoegl et al. [89].

10. SUPERPOSITION IN ANISOTROPIC MATERIALS.

Linear *isotropic* materials require *two* linear viscoelastic functions for a complete representation of all their time- or frequency-dependent mechanical properties. Anisotropic materials require more, Tschoegl [2]. *Axisymmetric* or *transversely isotropic* materials require five, and *orthotropic* or *orthorhombic* materials need *nine* functions. Many industrially important materials exhibit one or the other form of anisotropy. Drawn fibers are axisymmetric. Films produced by drawing, or by rolling, in a single direction are orthotropic. Two of the axisymmetric functions and three of the orthotropic ones describe bulk properties. The full linear viscoelastic

characterization of anisotropic materials is thus a daunting task and relatively little information on their time-dependent behaviour is available. Ward [90] includes a chapter on Anisotropic Mechanical Behaviour with a number of useful references. We conjecture that the effects of time and/or pressure on the manifold response functions of anisotropic materials may also be described by the WLF or the FMT models, provided that the functions are linearly viscoelastic. However, there is no satisfactory evidence on this issue one way or another.

11. CONCLUDING REMARKS AND RECOMMENDATIONS.

In the following, we summarize the salient points of this review and point out some areas in which work is currently lacking.

- We attempted to critically review models that deal with the superposition of the effect of time, temperature, and pressure in thermo- and/or piezo-rheologically simple polymeric materials. Our primary interest is the effect of pressure. However, we also reviewed the effect of temperature as necessary background. Pressure has an analogous, but opposite effect to that of temperature. Thus, the behavior under high pressure is roughly equivalent phenomenologically to the behavior at low temperature, and *vice versa*.

- The FMT model appears to predict most satisfactorily and most simply the combined effect of pressure and of temperature on single-transition polymers in thermodynamic equilibrium, i.e., on thermo- and piezo-rheologically simple materials. The FMT model reduces to the WLF model at the reference (usually the atmospheric) pressure. The former therefore comprises the latter as a special case. At the reference temperature the FMT model becomes formally analogous to the FS model. This model therefore handles time-temperature, time-pressure, and time-temperature-pressure superposition equally well. Being based on the free volume concept, the semi-empirical molecular parameters of the FMT model are the fractional free volume in the reference state, f_0, the expansion coefficient of the fractional free volume, $\alpha_f(P)$ at the pressure P, and the proportionality factor, B, of the Doolittle equation. At pressures other than atmospheric, the parameters of the occupied volume, K_ϕ^* and k_ϕ, are also required. Performing experiments based on temperature variation alone is not sufficient to calculate correct values of f_0 and α_f, since the value for B must be pre-assumed. When the measurements are executed as function of pressure as well as temperature, the value of B, f_0 and α_f as well as K_ϕ^* and k_ϕ, become uniquely determined.

- Time-temperature-pressure superposition is intrinsically unavailable for multi-phase and multi-transition materials. It may therefore not be strictly applicable to *any* polymeric material since secondary transitions are always present. Therefore, renewed efforts must be made to extend the *experimental window* through which materials are viewed, as well as the accuracy with which the measurements are performed.

- The traditional way of extending the experimental window is the combination of measurements made as functions of the time and of the frequency. Such

measurements must be converted into one another using an interconversion algorithm. See, for instance, Baumgaertel and Winter [91] on converting dynamic data, or Tschoegl and Emri [85, 86] and Emri and Tschoegl [92, 93, 94] on a rather more general method.

- Combining measurements made in the frequency as well as in the time domain is often unsatisfactory because of small variations in specimen properties and/or initial and boundary conditions (such as temperature, pressure, and/or humidity) if the measurements are not made on the same specimen and under the same experimental conditions. Tschoegl et al. [89] have proposed a Standard Protocol to be followed in such measurements. This is particularly important with any of the time-dependent *bulk* properties. These are critically dependent on highly accurate measurements because of their weak dependence on time or frequency.
- To extend the width of the experimental window there is a very definite need for the development of novel apparatus in which measurements may be performed in the frequency as well as in the time domain on the *same sample* and under *identical experimental conditions* by simply throwing a switch, as it were. The development of such an apparatus is within the capability of present day technology and should be undertaken forthwith.
- The effect of temperature and/or pressure on the mechanical properties of polymeric materials in the general case requires the construction of *contour plots*. Such plots will, however, be truly useful only if the data can span a sufficiently wide swath of the time and/or the frequency scale. The computer program employed for the construction of a contour plot should allow the user to recover at will the effect of temperature or pressure at a selected time or frequency, or the effect of time or frequency at a selected temperature or pressure. Programs of this kind are now available.
- We recommend the compilation of the parameters of the FMT equation on a number of the more important polymeric materials. Since this work will entail a determination of the pre-exponential factor, B, it will at the same time allow re-examination of the parameters of the WLF equation for the same materials. This work has now been initiated by Kralj et al. [1] and Emri and Prodan [62].
- The problem whether the superposition of the bulk properties follows the same rules (the WLF and/or the FMT equation) as do the shear properties should be resolved unambiguously. It is now almost universally accepted that the superposition of tensile properties follows the same rules as does that of the shear properties. If bulk behavior follows different rules, the tensile behaviour must be re-examined.
- Another unresolved problem is that of the time-pressure superposition of the mechanical properties of polymers in the glassy region, i.e., above P_g [42].
- Finally, the emerging technology of multi-component injection molding requires knowledge of the effects of temperature and pressure *variation* on each component upon cooling. This affects the mechanical, optical, electrical, and possibly other physical properties of the assembly.

13. APPENDIX.

13.1 Determination of the WLF Constants.

The WLF constants are obtained from segments of the relaxation curve measured at constant pressure and different temperatures, T_i, $i = 1,2,3,\cdots,N$, within an experimental window. A master curve is then obtained by shifting these segments along the logarithmic time scale by the distance $\log a(T_i)$. Thus, we obtain a set of discrete datum points:

$$\{\log a(T_i),\ T_i;\ i = 1,2,3,\cdots,N\}, \qquad \text{..... (126)}$$

which may be modeled with the WLF equation. The latter may be rearranged as:

$$Z = \frac{T - T_0}{\log a_T} = -\frac{1}{c_1^0}(T - T_0) - \frac{c_2^0}{c_1^0}, \qquad \text{..... (127)}$$

where Z is a linear function of the temperature difference, $T - T_0$, and T_0 is the chosen reference temperature. This relation is schematically shown in figure 13. The set of discrete data, equation (126), may be expressed as:

$$\{Z_i, \Delta T_i;\ i = 1,2,3,\cdots,N\}\ , \qquad \text{..... (128)}$$

where:

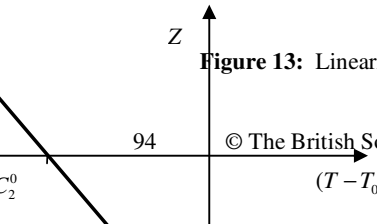

Figure 13: Linearized form of the WLF equation.

$$Z_i = \frac{T_i - T_0}{\log a(T_i)} = \frac{\Delta T_i}{\log a(T_i)}. \qquad \text{..... (129)}$$

Each discrete value Z_i may be modeled with the WLF equation, equation (11), as:

$$Z_i = Z(\Delta T_i) + \delta_i = -\frac{1}{c_1^0}\Delta T_i - \frac{c_2^0}{c_1^0} + \delta_i, \qquad \text{..... (130)}$$

where δ_i is the approximation error of modeling the Z_i with the WLF equation. Introducing the notation $a = -1/c_1^0$ and $b = -c_2^0/c_1^0$ we can re-write equation (130) as:

$$Z_i = Z(\Delta T_i) + \delta_i = a\,\Delta T_i + b + \delta_i, \qquad \text{..... (131)}$$

from which we find the approximation error for each Z_i as:

$$\delta_i = Z_i - (a\,\Delta T_i + b). \qquad \text{..... (132)}$$

Furthermore, we may write:

$$\Lambda = \sum_{i=1}^{N} \delta_i^2 = \sum_{i=1}^{N} [Z_i - (a\,\Delta T_i + b)]^2. \qquad \text{..... (133)}$$

Minimizing the sum of the squares with respect to *a* and *b* we obtain:

$$\frac{\partial \Lambda}{\partial a} = -2\sum_{i=1}^{N} [Z_i - (a\,\Delta T_i + b)]\Delta T_i = 0. \qquad \text{..... (134)}$$

After some rearrangement we get:

$$\begin{bmatrix} \sum_{i=1}^{N} \Delta T_i^2 & \sum_{i=1}^{N} \Delta T_i \\ \sum_{i=1}^{N} \Delta T_i & N \end{bmatrix} \begin{Bmatrix} a \\ b \end{Bmatrix} = \begin{Bmatrix} \sum_{i=1}^{N} Z_i\,\Delta T_i \\ \sum_{i=1}^{N} Z_i \end{Bmatrix}. \qquad \text{..... (135)}$$

The solution of this matrix equation is given by:

$$a = \frac{D_a}{D}, \text{ and } b = \frac{D_b}{D}, \qquad \text{..... (136)}$$

where:

$$D = \begin{vmatrix} \sum_{i=1}^{N} \Delta T_i^2 & \sum_{i=1}^{N} \Delta T_i \\ \sum_{i=1}^{N} \Delta T_i & N \end{vmatrix}, \qquad \text{..... (137)}$$

$$D_a = \begin{bmatrix} \sum_{i=1}^{N} Z_i \, \Delta T_i & \sum_{i=1}^{N} \Delta T_i \\ \sum_{i=1}^{N} Z_i & N \end{bmatrix}, \qquad \ldots\ldots\ldots (138)$$

and

$$D_b = \begin{bmatrix} \sum_{i=1}^{N} \Delta T_i^2 & \sum_{i=1}^{N} Z_i \, \Delta T_i \\ \sum_{i=1}^{N} \Delta T_i & \sum_{i=1}^{N} Z_i \end{bmatrix}. \qquad \ldots\ldots\ldots (139)$$

Solving the above determinants we find the constants c_1^0 and c_2^0 to be given as:

$$c_1^0 = -\frac{1}{a} = \frac{\left(\sum_{i=1}^{N} \Delta T_i\right)^2 - N \sum_{i=1}^{N} \Delta T_i^2}{N \sum_{i=1}^{N} Z_i \, \Delta T - \left(\sum_{i=1}^{N} Z_i\right) \sum_{i=1}^{N} \Delta T_i}, \qquad \ldots\ldots\ldots (140)$$

and

$$c_2^0 = \frac{b}{a} = \frac{\left(\sum_{i=1}^{N} \Delta T_i^2\right) \sum_{i=1}^{N} Z_i - \left(\sum_{i=1}^{N} Z_i \, \Delta T_i\right) \sum_{i=1}^{N} \Delta T_i}{N \sum_{i=1}^{N} Z_i \, \Delta T - \left(\sum_{i=1}^{N} Z_i\right) \sum_{i=1}^{N} \Delta T_i}. \qquad \ldots\ldots\ldots (141)$$

ACKNOWLEDGEMENTS

This work was supported by the Ministry of Science, Education and Sports of the Republic of Slovenia.

The author gratefully acknowledges the cooperation of Aleš Kralj and Ted Prodan of the Center of Experimental Mechanics at the University of Ljubljana in assembling and excerpting references. Special thanks are due to Ted Prodan for preparing several of the figures.

REFERENCES

1. Kralj, A, Prodan, T and Emri, I, *J. Rheol.*, 45 (2001) 929-943.

2. Tschoegl, N W, "The Phenomenological Theory of Linear Viscoelastic Behavior", Springer-Verlag, Berlin, (1989).

3. Gross, B, "Mathematical Structure of the Theories of Viscoelasticity", Hermann et Cie., Paris, (1968).

4. Gross, B, *J. Appl. Phys.*, 40 (1969) 3397.

5. Fillers, R W and Tschoegl, N W, *Trans. Soc. Rheol.*, 21 (1977) 51-100.

6. Moonan, W K and Tschoegl, N W, *J. Polym. Sci., Polym. Phys. Ed.*, 23 (1985) 623-651.

7. Rusch, K C, *J. Macromol. Sci.-Phys.*, B2 (1968) 421-447.

8. Plazek, D J, *J. Polym. Sci.*, A2(6) (1968) 621-638

9. Fesko, D G and Tschoegl, N W, *J. Polym. Sci., Part C, Symposia*, 35 (1971) 51-69.

10. Fesko, D G and Tschoegl, N W, *Internat. J. Polym. Mater.*, 3 (1974) 51-79.

11. Kaplan, D and Tschoegl, N W, *Polym. Engrg. Sci.*, 14 (1974) 43-49.

12. Cohen, R E and Tschoegl, N W, *Trans. Soc. Rheol.*, 20 (1976) 153-169

13. Brinson, L C and Knauss,W G, *J. Mech. Phys. Solids*, 39 (1991) 859-880.

14. Brinson, L C and Knauss, W G, *J. Appl. Mech.*, 59 (1992) 730-737.

15. Caruthers, J M and Cohen, R E, *Rheol. Acta*, 19 (1980) 606-613.

16. Shen, M C and Eisenberg, A, *Prog. Solid State Chem.*, 3 (1966) 407-481.

17. Moonan, W K and Tschoegl, N W, *Macromolecules*, 16 (1983) 55-59.

18. Tschoegl, N W, "Fundamentals of Equilibrium and Steady-State thermodynamics", Elsevier, Amsterdam, (2000).

19. Gibbs, J A and DiMarzio, E A, *J. Chem. Phys.*, 28 (1958) 373-383.

20. DiMarzio, E A and Gibbs, J H, *J. Chem. Phys.*, 28 (1958) 807-813.

21. DiMarzio, E A. and Gibbs, J H, *J. Polym. Sci.*, 40 (1959) 121-131.

22. DiMarzio, E A and Gibbs, J H, *J. Polym. Sci.* A1 (1963) 1417-1428.

23. DiMarzio, E A and Gibbs, J H, *J. Res. Nat. Bur. Stand*, A68 (1964) 611-617.

24. DiMarzio, E A, Gibbs, J H, Fleming III, P D and Sanchez, I C, *Macromolecules*, 9 (1976) 763-771.

25. Gibbs, J A, "Modern Aspects of the Vitreous State", Butterworths, London, (1960).

26. Paterson, M S, *J. Appl. Phys.*, 35 (1964) 176-179.

27. Bianchi, U, *J. Phys. Chem.*, 69 (1965) 1497-1504.

28. Matheson, A J, *J. Chem. Phys.*, 44 (1966) 695-699.

29. Doolittle, A K and Doolittle, D B, *J. Appl. Phys.*, 28 (1957) 901-905.

30. Williams, M L, Landel, R F and Ferry, J D, *J. Amer. Chem. Soc.*, 77 (1955) 3701-3707.

31. Ferry, J D, "Viscoelastic Properties of Polymers", 3rd Ed., Wiley and Sons, New York, (1980).

32. Schwarzl, F R and Zahradnik, F, *Rheol. Acta*, 19 (1980) 137-152.

33. Bueche, F, *J. Chem. Phys.*, 36 (1962) 2940-2946.

34. Bestul, A B and Chang, S S, *J. Chem. Phys.*, 40 (1964) 3731-3733.

35. Chang, S S, Bestul, A B and Horman, J A, in *Proceedings of the VII International Congress on Glass*, Brussels, (1965).

36. Goldstein, M, *J. Chem. Phys.*, 39 (1963) 3369-3374.

37. Adam, G and Gibbs, J H, *J. Chem. Phys.*, 43 (1965) 139-146.

38. Kauzmann, W, *Rev. Mod. Phys.*, 14 (1942) 12–44.

39. Eisenberg, A and Saito, S, *J. Chem. Phys.*, 45 (1966) 1673-1678.

40. Hutchinson, J M and Kovacs, A J, *J. Polym. Sci.: Polym. Phys. Ed.*, 14 (1976) 1575-1590.

41. Moonan, W K and Tschoegl, N W, *Internat. Polym. Mater.*, 10 (1984) 199-211.

42. Prodan, T, 'The effect of pressure and temperature on the shear relaxation behaviour of time-dependent materials', Ph.D. Thesis, Department of Mechanical Engineering, University of Ljubljana, Slovenia, (2002).

43. Bridgman, P W, "The Physics of High Pressure", G. Bell and Sons, London, (1949).

44. Gee, G, *Polymer*, 7 (1966) 177-191.

45. Havliček, I, Ilavsky, M and Hrouz, J, J. *Macromol. Sci. Phys,* B21 (1982) 425-441.

46. Ferry, J D and Stratton, R A, *Kolloid-Z.*, 171 (1960) 107-111.

47. McKinney, J E and Belcher, H V, *J. Res. Nat. Bur. Stand.*, 67A (1963) 43-53.

48. Tribone, J J, O'Reilly, J M and Greener, J, *J. Polym. Sci.: Part B: Polym. Phys.*, 27 (1989) 837-857.

49. Freeman, B D, Bokobza, L and Monnerie, L, *Polymer,* 31 (1990) 1045-1050.

50. O'Reilly, J M, *J. Polym. Sci.*, 57 (1962) 429-444.

51. O'Reilly, J M, Tribone, J J and Greener, J, *Polym. Sci., Polym. Phys. Ed.*, 26 (1988) 501-513.

52. Ramos, A R, Kovacs, A J, O'Reilly, J M, Tribone, J J and Greener, J, *J. Polym. Sci., Polym. Phys. Ed.*, 26 (1988) 501-513.

53. Tait, P, "Physics and Chemistry of the Voyage of H.M. Ship Challenger", Vol. II, Cambridge University Press, Cambridge, (1900).

54. Boldizar, A, Kubát, J and Rigdahl, M, *J. Appl. Polym. Sci.*, 39 (1990) 63-71.

55. Simha, R and Somcynsky, T, *Macromolecules*, 2 (1969) 342-350.

56. Simha, R and Wilson, P S, *Macromolecules*, 6 (1973) 902-913.

57. Somcynsky, T and Simha, R, *J. Appl. Phys.*, 42 (1971) 4545-4548.

58. Curro, J G, Lagasse, R R and Simha, R, *J. Appl. Phys.*, 52 (1981) 5892.

59. Utracki, L A, *Polym. Engrg. Sci.*, 23 (1983) 446-451.

60. Utracki, L A, *Polym. Prep., Amer. Chem. Soc.*, 24 (1983) 113.

61. Murnaghan, F D, *"Finite Deformation of Elastic* Solids", Wiley, New York, (1951).

62. Emri, I, Prodan, T, Submitted to *Experimental Mechanics*, (2004)

63. Stacer, R G and Husband, D M, *Rheol. Acta*, 29 (1990) 152-162.

64. Duperray, B and Leblanc, J L, *Kautschuck + Gummi · Kunststoffe*, 35 (1982) 298-307.

65. McCrum, N G, *Polymer*, 25 (1984) 309-317.

66. McCrum, N G and Morris, E L, *Proc. Roy. Soc.*, A281 (1964) 258-273.

67. McCrum, N G, Read, B E and Williams, G, "Anelastic and Dielectric Effects in Polymeric Solids", Wiley and Sons, New York, (1967).

68. Rusch, K C, *J. Macromol. Sci.-Phys.*, B2 (1968) 179-204.

69. Rusch, K C, *J. Macromol. Sci.-Phys.*, B2 (1968) 421-447.

70. Emri, I, Knauss, W G and Tschoegl, N W, 'Non-equilibrium time-dependent behaviour of polymeric materials', (2005), in preparation.

71. Tool, A Q, *J. Amer. Ceram. Soc.*, 29 (1946) 240-253.

72. Kovacs, A J, *Adv. Polym. Sci.*, 3 (1964) 394-507.

73. Knauss, W G and Zhu, W D, Mech. Time-Dependent Mater., (2002), to appear.

74. Wunderlich, B, "Macromolecular Physics, Volume I, Crystal Structure, Morphology, and Defects", Academic Press, New York, (1973).

75. Aharoni, S M, "n-Nylons: Their Synthesis, Structure and Properties", J. Wiley & Sons, Inc. New York, (1997), and references therein.

76. Eder, G, Janeschitz-Kriegl, H and Liedauer, S, Progr. Polym. Sci. 15(1990), 629-714.

77. Eder, G and Janeschitz-Kriegl, H, "Structure Development During Processing: Crystallization", In H.Meijer (ed.), Materials Science and Technology, Volume 18, Verlag Chemie, (1997).

78. Hearle, J W S, "Fiber formation and the science of complexity; In: Salem, D.R., Structure Formation in Polymer Fibers", Carl Hanser Verlag, (2001).

79. Swartjes, F H M, "Flow induced crystallization in elongation flow", Ph.D. thesis, Eindhoven Univeristy of Technology, (2001), downloadable from: www.mate.tue.nl.

80. Emri, I, and von Bernstrorff, B S, Submitted to *J. Appl. Mech*., (2004).

81. Cevc, P, Arčon, D, Blinc, R, and Emri, I, "Electron Paramagnetic Resonance of Stressed Fiber Nylon 6: Annealing Effects", In preparation, (2005).

82. Tobolsky, A V, "Properties and Structure of Polymers", Wiley and Sons, New York, (1960).

83. McLaughlin, J R and Tobolsky, A, *J.Colloid Sci*, 7 (1952) 555-568.

84. Plazek, D J, *J. Phys. Chem.*, 69 (1965) 3480-3487.

85. Tschoegl, N W and Emri, I, *Internat. J. Polym. Mater.*, 18 (1992) 117-127.

86. Tschoegl, N W and Emri, I, *Rheol.* Acta, 32 (1993) 322-327.

87. Deng, T H and Knauss, W G, *Mech. Time-Dependent. Mater.*, 1 (1997) 33-49.

88. Sane, S and Knauss, W G, *Mech.Time-Dependent Mater.*, 5 (2001) 293-324.

89. Tschoegl, N W, Knauss, W G and Emri, I, *Mech. Time-Dependent. Mater.*, 6 (2002) 3-51.

90. Ward, I M, "Mechanical Properties of Solid Polymers", Wiley-Interscience, London, (1971).

91. Baumgaertel, M and Winter, H H, *Rheol. Acta*, 28 (1989) 511-519.

92. Emri, I and Tschoegl, N W, *Rheol. Acta*, 32 (1993) 311-321.

93. Emri, I and Tschoegl, N W, *Rheol. Acta*, 33 (1994) 60-70.

94. Emri, I and Tschoegl, N W, *Internat. J. Polym. Mater.*, 40 (1998) 55-79.

